Nanostructured $CuFe_2O_4$ Spinel Catalysts Prepared By Flame Spray Pyrolysis for Hydrogen Production

By

Nutcha Anurak

A Thesis Submitted in Partial Fulfillment of the Requirements for the Degree

MASTER OF ENGINEERING

Department of Chemical Engineering

Graduate School

SILPAKORN UNIVERSITY

2011

Nanostructured $CuFe_2O_4$ Spinel Catalysts Prepared by Flame Spray Pyrolysis for Hydrogen Production

By

Nutcha Anurak

A Thesis Submitted in Partial Fulfillment of the Requirements for the Degree

MASTER OF ENGINEERING

Department of Chemical Engineering

Graduate School

SILPAKORN UNIVERSITY

2011

ตัวเร่งปฏิกิริยาคอปเปอร์เฟอร์ไรท์สปินเนลเตรียมโดยเฟลมสเปรย์ไพโรไลซิสในการเร่งปฏิกิริยารีฟอร์มมิ่งเพื่อผลิตไฮโดรเจน

โดย

นางสาวณัฐชา อนุรักษ์

วิทยานิพนธ์นี้เป็นส่วนหนึ่งของการศึกษาตามหลักสูตรปริญญาวิศวกรรมศาสตรมหาบัณฑิต
สาขาวิชาวิศวกรรมเคมี
ภาควิชาวิศวกรรมเคมี
บัณฑิตวิทยาลัย มหาวิทยาลัยศิลปากร
ปีการศึกษา 2554

The Graduate School, Silpakorn University has approved and accredited the Thesis title of "Nanostructured $CuFe_2O_4$ spinel catalysts prepared by flame spray pyrolysis for hydrogen production" submitted by Miss Nutcha Anurak as a partial fulfillment of the requirements for the degree of Master's of Chemical Engineering.

....
(Assistant Professor Panjai Tantatsanawong ,Ph.D.)
Dean of Graduate School

.........../......................./.............

Thesis Advisor

1. Assistant Professor Okorn Mekasuwandumrong, D.Eng.
2. Kajornsak Faungnawakij, Ph.D.

Thesis Examination Committee

.... Chairman
(Assistant Professor Choowong Chaisuk, D.Eng.)

.........../......................./.............

.... Member	.... Member
(Assistant Professor Joongjai Panpranot, Ph.D.)	(Suwimol Wongsakulphasatch ,D.Eng.)
.........../......................./.............	........../......................./..............
.... Member	.... Member
(Kajornsak Faungnawakij, Ph.D.)	(Assistant Professor Okorn Mekasuwandumrong, D.Eng.)
.........../......................./.............	.........../......................./..............

52404203 : MAJOR : CHEMICAL ENGINEERING

KEY WORDS : METHANAL STREAM REFORMING/ FLAME SPARY PYROLYSIS/ COPPER BASE SPINEL

NUTCHA ANURAK : NANOSTRUCTURED COPPER FERRITE SPINEL CATALYSTS PREPARED BY FLAME SPARY PYROLYSIS FOR HYDROGEN PRODUCTION. THESIS ADVISORS : ASST.PROF.OKORN MEKASUWANDUMRONG, D.Eng., AND KAJORNSAK FAUNGNAWAKIJ, Ph.D.. 89 pp.

Hydrogen fuel cells have been recognized as high efficient technologes for electricity generation with low pollution. Catalytic reformining of oxyhydrocarbon is a common process to produce hydrogen feed for fuel cells. Nanostructured $CuFe_2O_4$ spinel catalysts have been developed by one-step flame spray pyrolysis (FSP) method, and were tested for methanol stream reforming in a temperature range of 200 to 375 ^oC. The $CuFe_2O_4$ spinel catalysts were characterized by X-ray powder diffraction, temperature-program reduction, nitrogen adsorption, and transmission electron microscopy. The copper spinel nanoparticles with narrow particle size distribution in a range of 10-20 nm were successfully synthesized by FSP. The copper spinel catalysts exhibited a high activity and selectivity in steam reforming; the gaseous products were mainly hydrogen and carbon dioxide with a small amount of CO. Especially, the $CuFe_2O_4$ catalyst prepared at the ratio of Cu:Fe precursor of 1:2 showed the highest activity among the catalysts prepared at various Cu:Fe precursor ratios. With varied reduction temperatures of 200, 250, 300 and 350 ^oC, the $CuFe_2O_4$ reduced at 300 ^oC provided superior catalytic activity in methanol reforming.

Program of Department of Chemical Engineering Graduate School, Silpakorn University Academic Year 2011

Student's signature ....

Thesis Advisors' signature 1. .... 2. ....

52404203 : สาขาวิชาวิศวกรรมเคมี
คำสำคัญ : เมทานอล สตรีมรีฟอร์มมิ่ง/ เฟลมสเปรย์ไพโรไลซิส/ คอปเปอร์เบสสปิเนล

ณัฐชา อนุรักษ์ : ตัวเร่งปฏิกิริยาคอปเปอร์เฟอร์ไรท์สปินเนลเตรียมโดยเฟลมสเปรย์ไพโรไลซิสในการเร่งปฏิกิริยารีฟอร์มมิ่งเพื่อผลิตไฮโดรเจน
อาจารย์ที่ปรึกษาวิทยานิพนธ์: ผศ.ดร.โอกร เมฆาสุวรรณดำรงและ ดร.ขจรศักดิ์ เฟื่องนวกิจ 89 หน้า

เซลล์เชื้อเพลิงไฮโดรเจนเป็นที่รู้จักกันในเรื่องของเทคโนโลยีการผลิตไฟฟ้าคุณภาพสูง อีกทั้งยังมีมลพิษต่ำ ตัวเร่งปฏิกิริยารีฟอร์มมิ่งของออกซีไฮโดรคาร์บอนเป็นกระบวนการโดยทั่วไปในการผลิตไฮโดรเจนเพื่อเป็นสารตั้งต้นของเซลล์เชื้อเพลิง ตัวเร่งปฏิกิริยาสปินเนลที่มีโครงสร้างระดับนาโนคอปเปอร์เฟอร์ไรท์ได้ถูกพัฒนาขึ้นโดยใช้เฟลมสเปรย์ไพโรไลซิสในขั้นตอนเดียวและถูกตรวจสอบกับปฏิกิริยาเมทานอล สตีมรีฟอร์มมิ่งในช่วงอุณหภูมิ 200-375 องศาเซลเซียส ตัวเร่งปฏิกิริยาสปินเนลที่มีขนาดระดับนาโนคอปเปอร์เฟอร์ไรท์ได้ถูกตรวจสอบคุณลักษณะโดยใช้เครื่องตรวจสอบคุณลักษณะความเป็นผลึก เครื่องตรวจสอบพฤติกรรมการรีดิวซ์ เครื่องตรวจสอบการดูดซับโดยแก๊สไนโตรเจน และ กล้องจุลทรรศน์อิเลกตรอน จะเห็นว่าตัวเร่งปฏิกิริยาสปินเนลที่มีโครงสร้างระดับนาโนคอปเปอร์เฟอร์ไรท์ที่มีการกระจายตัวของรูพรุนที่แคบและมีขนาดอนุภาคอยู่ในช่วง 10-20 นาโนเมตรซึ่งเป็นความสำเร็จในการสังเคราะตัวเร่งปฏิกิริยาที่มีอนุภาคระดับนาโนโดยใช้วิธีเฟลมสเปรย์ไพโรไลซิสในขั้นตอนเดียว ตัวเร่งปฏิกิริยาสปินเนลที่มีโครงสร้างระดับนาโนคอปเปอร์เฟอร์ไรท์แสดงให้เห็นว่ามีประสิทธิภาพในการเร่งปฏิกิริยา และการเลือกเกิดของปฏิกิริยาสตรีมรีฟอร์มมิ่งสูง ซึ่งผลิตภัณฑ์ที่เกิดขึ้น นั่นคือ แก๊สไฮโดรเจน และ แก๊สคาร์บอนไดออกไซด์ โดยมีแก๊สคาร์บอนมอนอกไซด์เกิดขึ้นเล็กน้อย โดยเฉพาะอย่างยิ่งตัวเร่งปฏิกิริยาสปินเนลที่มีขนาดระดับนาโนคอปเปอร์เฟอร์ไรท์ที่เตรียมในอัตราส่วน 1:2 มีความสามารถในการเร่งปฏิกิริยาสูงที่สุด

ภาควิชาวิศวกรรมเคมี บัณฑิตวิทยาลัย มหาวิทยาลัยศิลปากร ปีการศึกษา 2553
ลายมือชื่อนักศึกษา..
ลายมือชื่ออาจารย์ที่ปรึกษาวิทยานิพนธ์ 1. .... 2. ....

ACKNOWLEDGEMENTS

The author would like to express her sincere gratitude and appreciation to her advisor, Assistant Professor Okorn Mekasuwandumrong, D.Eng. and co advisor, Dr. Kajornsak Faungnawakij for providing guidance and valuable advice throughout this research and devotion to revise this thesis.

In particular, the author would also be grateful to Assistant Professor Choowong Chaisuk, as the chairman, Dr. Suwimol Wongsakulpesutch and Assistant Professor Joongjai Panpranot as the members of the thesis committee. The author would like to thank the National Nanotechnology Center (NANOTEC) for the instrument supports. The author would like to thank Silpakorn University and the National Nanotechnology Center (NANOTEC) for the financial supports.

Most of all, the author would like to express her highest gratitude to her parents who always pay attention to us all the time for suggestions, supports and encourangements. The most success of graduation is devoted to her parents.

Finally, the author is qrateful to all of members of the National Nanotechnology Center (NANOTEC) for their assistances.

.

Table of Contents

Page

Chapter

Table of Contents

Page

Table of Contents

List of Tables

List of Figures

List of Figures

List of Figures

.

CHAPTER I

INTRODUCTION

1.1 Rationale

Combustion process for energy production has been developed, and used in our society for a long time. Nevertheless, the disadvantage is that a significant toxic gas (CO_x, NO_x and SO_x) is produced along with energy /power obtained. Toxic gases are causing toxicity to humans and the environment seriously. In addition, CO_2 would bring about global warming problem, while crude oil resources are limited. So, engine oil, gasoline and diesel must be replaced by alternative energy sources. Fuel cell has been developed to produce continuous electricity for the future. Also, fuel cell is recognized as the machine energy efficient and environmental friendly because the fuel cell can convert chemical energy into electrical energy by electrochemical reactions at the electrodes of fuel cell and oxygen through electrolyte. This produce only water and heat on the side production (figure 1.1). A typical fuel used in fuel cells is hydrogen while the oxygen comes from the air**.** Also, hydrogen is used as a reactant in hydrogenation reaction for important industrial process since it produces a value able product for the chemical manufacture of different compounds and synthetic fuel.

Now, the prices per unit of hydrogen from fossil energy sources such as LPG have a very high price as well as a complicated process. Nevertheless, production of hydrogen from renewable energy sources such as methanol, ethanol and dimethyl ether, etc., is still in the early stages of development and needs to be further developed for actual utilization.

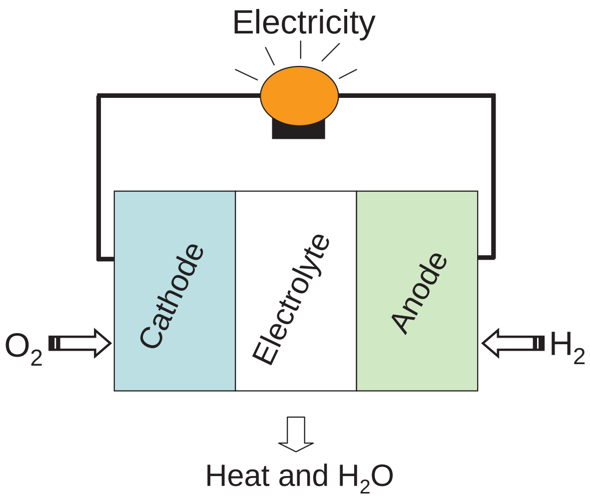

Figure 1.1 Components and operating principles of fuel cells.

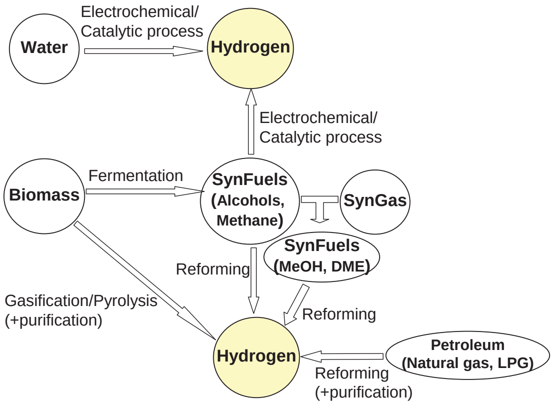

Figure 1.2 The various technologies involved in the production of hydrogen.

Hydrogen production process can be achieved through a process of many types, biomass gasification/pyrolysis, water–splitting and reforming of the various fuels (Figure 1.2). Hydrogen production process that is receiving currently attention and development for fuel cell applications is reforming process; a process that can produce hydrogen continuously and sufficiently. In general, the reforming process requires its suitable catalyst such as methanol reforming on a copper catalyst and dimethyl ether reforming on a copper and alumina catalyst. Methanol and the dimethyl ether is a substance that can be produced from biomass. The reforming reaction of methanol and dimethyl ether are shown in reaction 1 and 2, respectively.

Methanol reforming : $CH_3OH + H_2O \rightarrow 3H_2 + CO_2$ (1)

Dimethyl ether reforming : $CH_3OCH_3 + 3H_2O \rightarrow 6H_2 + 2CO_2$ (2)

In addition to these primary reactions, some side reactions could occur and affect the quality of the hydrogen reformate because side-product impurities such as carbon monoxide and methane. This can decrease the performance of the fuel cell. Therefore it is necessary to increase the hydrogen purification process to increase productivity and eliminate impurity. Some side reactions could deteriorate the reforming catalyst. The reaction conditions are also highly influencing the activity, selectivity and stability of catalysts.

Spinel structure catalysts can be used as catalysts in the dimethyl ether and methanol reforming reaction. It has the potential to be used commercially in the future. However, due to sintering and coking, it has to be further developed to enhance the stability of the catalyst. Therefore, it is necessary to study and develop the composition and properties of the catalysts to qualifications as needed. General production process can produce catalyst with large particle size in micron scale and the surface area is very low (less than 1 square meters per gram). Therefore, development of synthesis technology to the nanoscale structures such as nano-sized particles will provide the catalyst to have a special feature both in terms of activity and stability. The promising technology for the synthesis of spinel catalysts is one-step flame spray pyrolysis for spinel nano-particles formation.

In flame spray pyrolysis (FSP), the metal precursor is a combustible liquid that is sprayed and ignited, resulting in nano-particles in large quantities [1] such as fume silica, titania, and carbon black in large quantity at low cost. The applications of supported metal catalysts synthesized via one-step flame spray pyrolysis have been reported. For examples, flame-made Pt-Ba/Al_2O_3 and Pt/Ba/$Ce_xZr_{1-x}O_2$ have been investigated in lean-NO_x storage-reduction [2, 3]. High surface area Ag/ZnO prepared by flame spray pyrolysis has been reported to exhibit high photocatalytic performance in UV-photo degradation of methylene blue [4]. Recently, Sukanya et al. [5] successfully applied the flame spray pyrolysis method for synthesis of various Al_2O_3 supported noble metal catalysts such as platinum and tin. The flame spray pyrolysis catalysts exhibited superior catalytic activity and better stability than the ones made by impregnation in the dehydrogenation of propane[6].

1.2 Objectives

The objective of this research is to synthesize spinel nanostructure by flame spray pyrolysis. The effect of precursor feed flow rate, precursor concentration and composition of metal precursors for primary condition on the synthesized catalysts was studied. Also the reduction temperature of the resultant catalyst investigated in hydrogen production reaction via methanol steam reforming and dimethyl ether steam reforming.

1.3 Research Scopes

Preparation condition

- Synthesis nano-crystalline $CuFe_2O_4$ catalysts by flame spray pyrolysis with loading ratio of Cu and Fe at 1:2.
- The particle size of flame-made $CuFe_2O_4$ catalysts was varied by changing the preparation condition ;
    1) Types of precursor are 1) metal nitrates, and 2) metal acetylacetonate mixed with metal nitrate in ethanol
    2) Precursor feed rate from 3 to 7 ml/min with loading ratio of Cu and Fe at 1:2.
    3) The concentration of precursor from 0.1 to 0.5 mole/liter with loading ratio of Cu and Fe at 1:2.

- Effect of ratio of Cu:Fe spinel catalyst: synthesis nano-crystalline $CuFe_2O_4$ catalysts by flame spray pyrolysis by loading ratio of Cu and Fe in 1:3, 1:2 and 1:1 in best precursor and in best condition.
- Effect of composition of Cu spinel catalyst: synthesis nano-crystalline $CuFe_2O_4$ catalysts by flame spray pyrolysis in best ratio of Cu: Fe by changing loading ratio of Fe and Mn at 0.5:1.5, 1.5:0.5, 0:2 and 2:0.
- Effect of temperature reduction of Cu spinel catalyst: synthesis nano-crystalline $CuFe_2O_4$ catalysts by flame spray pyrolysis in best ratio of Cu: Fe by changing reduction temperature in a range of 250-400°C for 60 min.
- Synthesis alumina nano-crystalline by for test in dimethyl ether steam reforming. Types of precursor are aluminum nitrate in ethanol and aluminum tri-sec-butoxide in xylene at the best condition.

Catalyst Characterization

1) X-ray diffraction (XRD)
2) Transmission Electron Microscope (TEM)
3) N_2 physisorption
4) Temperature Programmed Reduction (TPR)

Catalytic activity evaluation

- Study the catalytic performance of the flame-made catalysts such as activity and selectivity of hydrogen on methanol steam reforming reaction by varying the reaction temperature from 200-375°C.
- Compare performance of flame-made $CuFe_2O_4$ catalysts and reference $CuFe_2O_4$(commercial).
- Study the catalytic performance of the flame-made catalysts such as activity and selectivity of hydrogen on dimethyl ether steam reforming reaction by varying the reaction temperature from 200-375°C.

CHAPTER II

LITERATURE REVIEWS

2.1 Methanal and Dimethyl ether steam reforming

Verious types of hydrogen production systems have been extensively studied. Hydrogen is an environmentally friendly fuel since it does not release carbon dioxide on site when employed in fuel cell processor. Several hydrogen-generating techniques, i.e. steam reforming, partial oxidation, and autothermal reforming of various fuels, e.g. gasoline, LPG, methane (CH_4), methanol (MeOH), ethanol (EtOH), and dimethyl ether (DME), have been regarded as the efficient processes for deployment of fuel cell systems. Interestingly, dimethyl ether steam reforming (DME SR) is a two-step reaction namely dimethyl ether hydrolysis following by methanol steam reforming. Thermodynamic consideration forms any reactions for example dimethyl ether steam reforming and methanol steam reforming has been used to estimate the equilibrium product distribution as a function of the processing conditions. Dimethyl ether and methanol are suitable for on-board reforming because they can easily be liquefied and be reformed at low temperature of 200-350 ºC for methanol and 200-450 ºC for dimethyl ether. Presently, dimethyl ether is recognized as a promising alternative hydrogen source because dimethyl ether is less toxic and therefore is preferable to methanol. Development of catalysts for steam reforming reaction needs study appropriate condition can suppress such deactivation and coke formation [7, 8].

In the year 2006, K.Faungnawakij et al. studied thermodynamic analysis of dimethyl ether steam reforming and methanol steam reforming. In term of thermodynamic analysis of dimethyl ether steam reforming, the equilibrium calculation employing Gibbs free minimization was performed to figure out the required steam-to-carbon ratio (S/C = 0–5) and reforming temperature (25–1000ºC) where coke formation was thermodynamically unfavorable. S/C, reforming temperature and product species strongly contributed to the coke formation and product composition. When chemical species, dimethyl ether, methanol, CO_2, CO, H_2, H_2O and coke were considered, complete conversion of dimethyl ether and hydrogen yield above 78% without coke formation were achieved at the normal operating temperatures of molten carbonate fuel cell (600 ◦C) and solid oxide fuel cell (900 ◦C), when S/C was at or above 2.5. When methane was favorable, production of coke and that of hydrogen were significantly suppressed [7]. Furthermore, in term of thermodynamic equilibrium of steam reforming process of methanol, influence of steam-to-carbon ratio (S/C = 0–10), reforming temperature (25–1000 ◦C), and pressure (0.5–3 atm) on conversion of fuels, hydrogen production, and CO formation has been figured out. Based upon a compound basis set methanol, CO_2, CO, H_2 and H_2O, complete conversion of methanol was attained at S/C=1 when the temperature was higher than 200 ℃ at atmospheric pressure. The concentration and yield of hydrogen could be achieved at almost 75% on a dry basis and 100%, respectively. From the reforming efficiency, the operating condition was optimized for the temperature range of 100–225 ◦C, S/C range of 1.5–3, and pressure at 1 atm. The calculation indicated that there forming condition required from sufficient CO concentration (<10 ppm) for polymer electrolyte fuel cell application is too severe for the existing catalysts (T_r =50 ◦C and S/C=4–5) [8].

Especially, in term of dimethyl ether steam reforming needs study effect of solid acids catalysts which dimethyl ether steam reforming is a two-step reaction namely dimethyl ether hydrolysis following by methanol steam reforming because solid acids catalysts can dimethyl ether dissociate to methanol. In the year 2007, K.Faungnawakij et al. showed a comparative study of the catalytic performance and the kinetic parameter of solid acids (Al_2O_3) derived from bayerite, γ-Al_2O_3, ZSM-5, H-mordenite, and TiO_2 in hydrolysis of dimethyl ether to methanol have been investigated. The stronger and the larger acid sites give rise to higher conversion in hydrolysis; however, fast degradation due to coking and low quality of product are observed. The acid strength of the solid acids is as follows: H-mordenite > ZSM-5 > PBT, ALO8 > TiO_2. The apparent activation energies of dimethyl ether hydrolysis over H-mordenite, ZSM-5, PBT, ALO8, and TiO_2 were determined as 73, 76, 101, 146, and 186 $kJmol^{-1}$, respectively. Furthermore, they studied steam reforming of dimethyl ether over composites of the solid acid and copper iron spinel was evaluated for hydrogen production. The optimum weight ratio of Cu spinel and alumina is in the range of 1:1 to 2:1 (Cu content = 13.3–17.7 wt %) to show a maximum reforming performance. And increasing the steam-to-carbon ratio obviously suppresses the catalyst degradation. Performance of composite catalysts of solid acid and Cu spinel in dimethyl ether steam reforming definitely depends on a dimethyl ether hydrolysis activity over the solid acid: namely, the high hydrolysis activity led to high steam reforming activity [9].

In addition, both of dimethyl ether steam reforming and methanol steam reforming are investigated the influences of type and preparation process of Cu spinels e.g. temperature reduction, temperature calcinations because the catalyst preparation process can affect the catalytic performance. Therefore, K.Faungnawakij et al. studied the preparation condition of the Cu-based spinel and that of alumina along with a mixing state of the composite catalyst to fine tune the optimal condition. The results showed that, a highly active composite was achieved when the calcinations temperature of the Cu spinel was at 900 °C and that of the alumina was at or below 700°C. The calcinations temperature strongly affected the crystallinity and reducibility of the copper ferrite spinel and the acidity of alumina and N.Shimoda et al. studied the effects of preparation conditions especially heat and reduction treatment of the $CuFe_2O_4$ spinel and γ-Al_2O_3. The result showed that, the heat treatment in air after mixing of $CuFe_2O_4$ and γ-Al_2O_3 improved the activity and durability of the composite catalysts for dimethyl ether steam reforming. The treatment temperature range of 700 – 800 °C is most effective to enhance the catalytic performance [10, 11].

Furthermore, dimethyl ether conversion and hydrogen production significantly depended on gas hourly space velocity (GHSV) and reforming temperatures (T_r). dimethyl ether conversion (>95%), hydrogen production rate (50 $molkgcat^{-1}h^{-1}$), and hydrogen concentration (ca.73%) were achieved at T_r of 350 °C and GHSV of 1500 h^{-1}. The maximum hydrogen production rate of 120 $molkgcat^{-1}h^{-1}$ was found at T_r of 450 °C and GHSV of 4000 h^{-1} [12]. Furthermore, the composite catalysts both with and without pre-reduction were active for dimethyl ether steam reforming when the pre-reduced catalyst exhibited higher initial activity. Investigation of hydrogen reduction pretreatment and metal doping to Cu–Fe spinel catalyst coupled with

γ–alumina was performed in dimethyl ether steam reforming for hydrogen production. The high activity and stability of the catalysts were achieved when the catalysts were reduced at or below 350 °C due to the stability of obtained Cu and Fe_3O_4 phases. Reduction at higher temperatures of 450 and 600 °C would bring about the decrease in activity and stability because the resultant Fe_3O_4 was further reduced to metallic Fe, and sintering of metallic Cu and Fe proceeded [11].

Besides improving conversion and hydrogen production, degradation also have an important role in development catalysts. K.Faungnawakij et al. studied the degradation behavior of the composites of $CuFe_2O_4$ and γ -Al_2O_3 in dimethyl ether steam reforming over a reaction time of 1000 h. The regenerability of degraded catalysts after the long-term tests also was investigated. The fresh, degraded, and regenerated composites were characterized to clarify the origin of deactivation and regeneration. Result show that, The durability of composite catalysts of $CuFe_2O_4$ and γ -Al_2O_3 was investigated during steam reforming of dimethyl ether. Partial degradation of the composites proceeded due to the concomitant effect of copper sintering and carbon formation. The catalyst degraded after steam reforming for 1100 h was regenerated by calcination in air in the temperature range of 500–700 °C; redispersion of copper via spinel formation and simultaneous carbon burning were achieved. The apparent activation energy for dimethyl ether steam reforming over the catalyst was estimated to be in the range of 150–160 $kJmol^{-1}$ and remained almost stable during the dimethyl ether steam reforming reaction test for 1100 h. Degradation of the catalyst was found to follow first-order kinetics with a deactivation rate constant of $0.95\times 10^{-3}\ h^{-1}$ [13].

In recent years, the composites of Cu-based spinel-oxide type and alumina or zeolite have been proposed for dimethyl ether steam reforming from our research group. A high dispersion of Cu species could be obtained from the spinel structure and would lead to an excellent catalytic performance. In normal spinels AB_2O_4, A is generally a divalent cation occupying tetrahedral sites, while B is a trivalent cation occupying octahedral sites. In inverse spinels, half of B occupies the tetrahedral sites, and the formula is rewritten as $B[AB]O_4$. Therefore, dopants (Mn, Cr, Co, and Al) could affect the reforming performance in terms of both activity and selectivity to products [11]. Moreover in year 2008, K.Faungnawakij et al. studied the effects of trivalent species (B site) in CuB_2O_4 spinels on dimethyl ether steam reforming performance. Crystallinity, reducibility, and oxidation states of the Cu-based spinels were evaluated. Catalytic performances in terms of dimethyl ether conversion, hydrogen yield and selectivity to carboncontaining species were measured and are discussed. Result show that, Cu-based spinel-oxides CuB_2O_4 (B = Fe, Mn, Cr, Ga, Al, or $Fe_{0.75}Mn_{0.25}$) were synthesized via a sol–gel method and subsequent solid-state reaction. The spinels mechanically mixed with γ-Al_2O_3 were evaluated for production of hydrogen from dimethyl ether steam reforming. The descending order of the activity was as follows: $CuFe_2O_4$, $CuFe_{1.5}Mn_{0.5}O_4 > CuAl_2O_4 > CuCr_2O_4 > CuMn_2O_4 > CuGa_2O_4$ while only $CuFe_2O_4$, $CuFe_{1.5}Mn_{0.5}O_4$, $CuCr_2O_4$, and $CuMn_2O_4$ were highly stable at reforming temperature of 350°C. The reduced phases of the Cu-based spinel catalysts that strongly affected the catalytic activity and durability were composed of metallic copper with metal oxides or with spinels. The stability of B metal oxides and the interaction between copper species and B metal oxides significantly contributed to the reforming performance [14].

Many papers emphasize that dimethyl ether steam reforming proceeds via consecutive two steps; dimethyl ether hydrolysis to methanol followed by steam reforming of methanol to hydrogen. It is generally known that acidic sites catalyze hydrolysis of dimethyl ether, and the Cu-based catalyst has high activity in the steam reforming of methanol So, Cu-based catalysts are improved in methanol steam reforming and Cu-based catalysts in dimethyl ether steam reforming can also refer with MeOH steam reforming [15]. In 2009, T.Fukunaga et al. investigated the activity of non-spinel CuMn mixed oxide to clarify the main factor of CuMn spinel catalyst for the high catalytic performance. The result showed that, CuMn-spinel oxide (CuMn(S)) and non- spinel CuMn mixed oxide (CnMn(NS)) have been obtained by calcining the same precursor at 900 °C and 300 °C respectively. The CuMn(S) consisted of $Cu_{1.5}Mn_{1.5}O_4$ spinel and Mn_3O_4, while CuMn (NS) consistedof CuO and Mn_3O_4. After reduction, Cu metal and MnO were observed on both catalysts and the Cu particle size was smaller on the CuMn (S) derived catalyst than the non-spinel. In methanol steam reforming, reduced CuMn(S) catalyst showed higher activity than the reduced CuMn

(NS) catalyst, due to the higher Cu metal dispersion [16]. If consider the optimum catalysts for methanol steam reforming or dimethyl ether steam reforming should also investigated water gas shift reaction because this reaction is side reaction of the both steam reforming reaction. Yohei Tanaka found that Mn/Fe ratio in the Cu–Mn–Fe catalysts influenced reducibility of copper oxide after reduction of spinel phases. Fe-rich Cu–Mn–Fe samples are considered to possess smaller Cu particles in smaller amounts than Mn rich catalysts. Optimized Cu/Mn/Fe ratio was 1:1:1 in terms of catalytic activity. Not only particle size and amount of Cu but also active supports are significant to improve WGSR activity [15]. From overall literature reviews can confirm Cu-based spinel shows excellent conversion and hydrogen production rate for MeOH steam reforming. Generally, copper and copper oxides are active for MeOH steam reforming but increasing reaction temperature also improved MeOH conversion.

A.Houteit et al. studied the promoting effect of alkaline compound like cesium and potassium on Cu/Al_2O_3 catalysts. The stability for hydrogen production from methanol steam reforming. The hydrogen formation is equal to the hydrogen thermodynamic value for 2 wt% of Cs. The increase in reaction temperature also improves methanol conversion. Hydrogen yield is quantitative in the temperature range 350–500 ºC for a CO concentration equivalent to less than 0.2 vol%. The results of XRD and XPS show that the addition of Cs oxide prevents copper oxide crystallites from sintering and the reduction into metallic Cu. Also, it inhibits the formation of $CuAl_2O_4$ spinel upon thermal treatment. It issuggested that high activity, selectivity and stability of Cs promoted catalysts result from a higher copper crystallites stability and the synergetic effect of cesium. [17]

2.2 Flame spray pyrolysis (FSP)

Flame aerosol technology is employed widely for large-scale manufacture of carbon blacks and ceramic commodities such as fumed silica and titania and to a lesser extent, for specialty chemicals such as zinc oxide and alumina powders [2]. However, by using a vapor-fed flame reactor it is often difficult to produce multicomponent materials with homogeneous chemical composition because differences in the chemical reaction rate and the vapor pressure of the reactants, nucleation and growth rates of the product may lead to non-uniform composition from particle to particle or even within a single particle.

In term of condition flame spray pyrolysis was studied. In 2003, Mueller et al. studied nanoparticle synthesis at high production rates of nanostructured silica particle by flame spray pyrolysis. A systematic investigation of flame spray synthesis of silica nanoparticles at high production rates up to 1.1kg/h was carried out using a commercially available external-mixing stainless-steel gas assisted atomizer. The influence of silica powder production rate, precursor concentration and oxidant dispersion gas flow rate was investigated on the product primary particle diameter, morphology and carbon content using hexamethyldisiloxane (HMDSO) in ethanol at 1.26 and 3.0 M as well as pure HMDSO (4.7 M). The average product primary particle size was controlled from 10 to 75 nm independent of precursor concentration confirming that particle formation can take place during flame spray pyrolysis in the gas phase following rapid evaporation of precursor droplets. The control of primary particle size (operation window) using flame spray pyrolysis was similar to that by the well-established vapor-fed aerosol reactors through the oxidant or precursor delivery rates. Limited variation of the product particle size was obtained when using air instead O_2 as dispersion gas (at constant pressure drop across the nozzle) or by providing additional sheath O_2 gas [18]. In year 2006, Hee Dong Jang et al. also studied the synthesis of SiO_2 nano-particles from sprayed droplets of tetraethylorthosilicate by the flame spray pyrolysis. TEOS concentration, maximum flame temperature, and residence time of reactants in the flame were chosen as key experimental variables for the control of the particle morphology, and average particle diameter. Larger particles were produced with decrease of the maximum flame temperature by controlling of hydrogen flow rate and oxygen in the burner. Average particle diameter increased with the increase of residence time by controlling the carrier gas flow rate [19].

Because Flame aerosol process has been used to produce various nanoparticles such as ceramic, metal and composite powders because it provides good control of particlesize, particle crystal structure and this method also can produce highly pure particles continuously without further subsequent process, for example, drying, calcinations and milling in the wet chemical processes. So many researchers studied flame spray synthesis of various nanoparticles with improved their reaction such as M. J. Height et al. studied Ag-ZnO catalysts. High specific surface area and crystalline Ag-ZnO photocatalysts were made by one-step flame spray pyrolysis. Result show that, flame-made Ag-ZnO showed higher photocatalytic activity than wet-made and reference titania powders. The photocatalytic performance was improved for flame-made materials made at longer high-temperature residence times in the flame. The latter particles exhibited improved crystallinity, as measured by UV–vis absorption and XRD [20]. Addition, S.Pisduangdaw et al. synthesis mono- and bi- metallic by flame spray pyrolysis of found that the flame spray pyrolysis catalysts exhibited superior catalytic activity and better stability than the ones made by impregnation in the dehydrogenation of propane when the Pt–Sn/Al_2O_3 catalysts prepared by conventional impregnation of Pt and Sn precursors on both the flame-synthesized and the reference Al_2O_3 were also employed for comparison purposes [6].

For this research, flame spray pyrolysis can synthesis spinel structure because the metal precursors evaporate in this spray flame and are combusted. The process features short residence times (a few milliseconds) and high maximum process temperatures (up to 3000K) such as Nielsvan Vegten et al. synthesis of $MgAl_{2-x}M_xO_4$ (M = Mn, Fe and Co, x = 0.1, 0.5, 1 and 2) spinel-like materials by flame-spray pyrolysis is presented. Mn, Fe and Co were chosen since these transition metals themselves form spinel phases readily and they show different activity for the combustion of methane, based on literature. The effect of the transition metal content on characteristics such as specific surface area and activity is discussed. Results show that, Spinel-like oxides, with the formula $MgAl_{2-x}M_xO_4$ ($x = 0.1$, 0.5, 1 and 2, M = Mn, Fe or Co) have been prepared by single step flame spray pyrolysis. These materials appeared single phase by X-ray diffraction. Electron microscopy showed the material to consist of mono crystalline particles of 6 to 15 nm in diameter. Aluminum free spinels ($x = 2$) possessed good initial activity in the catalytic combustion of methane, but the low thermal stability of these materials significantly reduced their catalytic applicability. By introducing Al ($x = 0.1$, 0.5 and 1), the initial activity decreased, but a concurrent increase in thermal stability resulted in materials [21].

CHAPTER III

THEORY

3.1 Copper based spinel

Copper ferrite crystallizes as a spinel structure. The spinel ferrite unit cell is based on a closed packed oxygen lattice, where metal cation reside on 8 of 64 tetrahedral sites (A-sites) and 16 of the 32 octahedral sites (B-sites). Spinel copper ferrite shows a remarkable variation in its atomic arrangement depending critically on the thermal history of the preparation and may be attributed to the distribution of Cu and Fe cations between the two nonequivalent lattice A and B sites. There are two types of spinel structure. Accordingly, the molecular formula of that ferrite can be written as

$$[Cu_{\delta}^{II}Fe_{1-\delta}^{III}]_{tetra}[Cu_{1-\delta}^{II}Fe_{1+\delta}^{III}]_{octa}O_4 \tag{3.1}$$

Where $\delta = 1$ for normal spinel

$\delta = 0$ for inverse or distorted spinel

The obtained type depends on the method of preparation and is variable with the preparation temperature and type of cations [22].

1) **Normal spinel**, the divalent metal ion occupies the tetrahedral site and the trivalent ion occupies the octahedral site. The general formula for an inverse spinel structure is given as AB_2O_4.

2) **Inverse or distorted spinel,** the cations may shift between the A and B sites. Half of the B cations go to the tetrahedral sites and the A cations go to octahedral interstices. The general formula for an inverse spinel structure is given as $B(AB)O_4$.

Ferrites of general formula MFe_2O_4 (where M denotes a divalent cation) are technologically important materials. Especially, $CuFe_2O_4$ is of long standing interest in solid state physics, mineralogy, ceramics and crystal changes due to the heat treatment. By virtue of magnetic and semiconducting properties, copper ferrite ($CuFe_2O_4$) and its solid solutions with other ferrites are widely used in the electronic industry. Copper ferrite has two crystallographic spinel structures: the high-temperature cubic phase (c-$CuFe_2O_4$) with a lattice parameter of 8.380 Å, and the low-temperature tetragonal phase (t-$CuFe_2O_4$) with lattice parameters of a 58.216 Å and c 58.709Å [23]. A summary of crystallographic properties of the two varieties is given in Table 3.1.

Apart from their technological importance as magnetic materials, ferrites also have well-established catalytic properties for many reactions such as oxidative dehydrogenation of hydrocarbons, decomposition of alcohols as well as good gas sensing properties and steam reforming reaction. All these properties strongly depend on their exact chemical composition and their microscopic physical structure.

Table 3.1 Crystallographic properties of copper ferrite spinel

Properties Crystal structure	Cubic	Tetragonal
Density, g/cm^3	5.414	5.405
Condition	high-temperature	low-temperature
Dimension		
a	8.380 Å	58.216 Å
b		
c		58.709Å

3.2 Flame spray synthesis method (FSP method)

Copper ferrites are usually prepared by a solution formed with cation stoichiometry of the desired ferrite; co-precipitation (with controlled conditions such as the pH and the concentration of the starting solutions) leads to a mixture of very small particles containing the cations in the right proportion. Additionally, the precipitation occurs by the removal of the solvent either by evaporation (spray-drying) or solidification and sublimation (freeze-drying) or by the addition of a different solvent (sol-gel).

In the case of molecular precursors, the technique is based on the preparation of a chemical compound (metal-organic molecule) containing the cations of the ferrite in the desired proportions (polynuclear coordination compounds). Using these methods, ferrite particles are obtained at relatively low temperatures. Particularly for the precursor method, the major advantages are:

(i) The control of stoichiometry in the powder,
(ii) The chemical homogeneity on atomic scale,
(iii) The high chemical purity and strain free without grinding,
(iv) The uniformity of oxide nano-particles with high surface area commonly exhibiting many unusual and interesting properties.

Moreover, new technique flame technology is a scalable, continuous and well-established method for the production of nanoparticles in large quantities[1]. The synthesis is based on metal loaded liquid precursors and achieves accurate control over the composition and size of the nanoparticles. High batch-to-batch reproducibility, a highly homogeneous product and a wide product variety are only a few of the useful attributes of flame spray synthesis. With this technology, there are manifold opportunities to take the developed technologies to industrial products.

3.2.1 Flame processes for catalyst preparation

Various aerosol reactors and methods have been developed for the synthesis of a wide variety of metal and metal oxide particles. Processes for aerosol flame synthesis are classified first depending on the precursor state fed to the flame in vapor-fed (VAFS) and liquid-fed aerosol flame synthesis (LAFS). In the latter, if the liquid precursor solution drives the flame process (contributes more than 50% of the energy) it is called flame spray pyrolysis. If a non-combustible solution is fed into the flame then LAFS is called flame-assisted spray pyrolysis (FASP), in Fig 2.2.

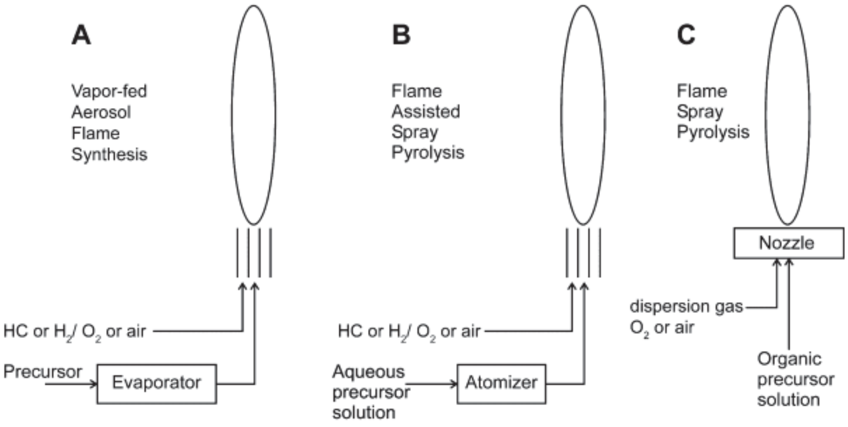

Figure 3.1 Schematic of selected flame configurations used for the synthesis of heterogeneous catalysts. (A)VAFS, (B) FASP and (C) FSP[1].

In flame spray pyrolysis, the metal precursors evaporate in this spray flame and are combusted. Particles are then formed by nucleation from the gas phase, in Fig.2.3. The process features short residence times (a few milli seconds) and high maximum process temperatures (upto3000K) [24]. The flame spray pyrolysis has been used for the synthesis of many different solid catalysts, such as Pt/Al_2O_3 [25], various perovskites [26], spinel structure [1], etc. Especially, Copper ferrites are prepared by flame spray pyrolysis because copper ferrite crystallizes as a spinel structure.

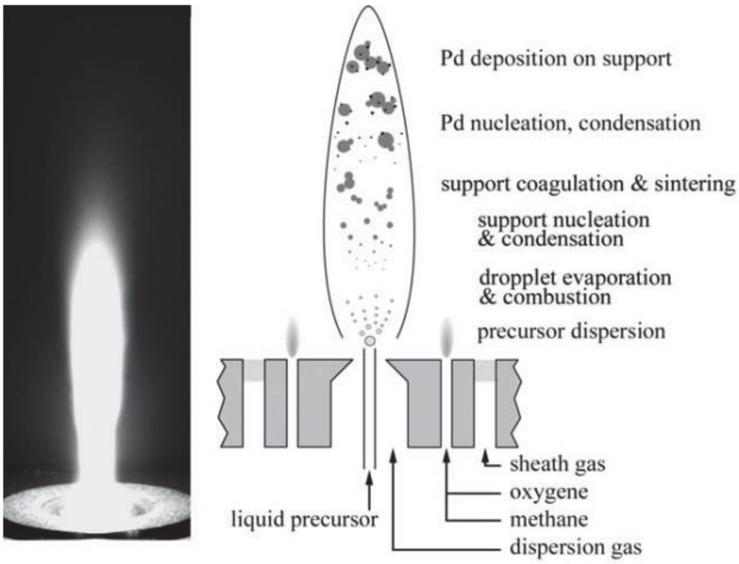

Figure 3.2 Sketch of the flame spray pyrolysis unit. The image shows a typical spray flame producing Pd/Al_2O_3 nanoparticles [27].

3.3 Methanol steam reforming (MeOH SR)

3.3.1 Hydrogen production from methanol

There are three process alternatives to produce hydrogen through the conversion of methanol:

1. **Decomposition**

   $CH_3OH \rightarrow 2H_2 + CO \quad \Delta H_r = 128$ kJ mol^{-1} (3.2)

2. **Partial oxidation**

   $CH_3OH + 0.5O_2 \rightarrow 2H_2 + CO_2 \quad \Delta H_r = -192$kJ mol^{-1} (3.3)

3. **Steam reforming**

   $CH_3OH + H_2O \rightarrow 3H_2 + CO_2 \quad \Delta H_r = 50$ kJ mol^{-1} (3.4)

However, the reaction is strongly endothermic which means that it requires a lot of energy for operating. Furthermore, the decomposition yields product gas containing up to 67% hydrogen and 33% carbon monoxide. The high content of CO requires a CO clean-up system if this reaction would be used in the fuel cell system. The CO clean-up system is regarded to be the most complicated part in the fuel cell system. Because of these drawbacks, the decomposition of methanol is found to be unsuitable for fuel cell applications. In contrast to the decomposition reaction, partial oxidation is a fast and exothermic reaction. The methanol steam reforming is known as a reverse reaction of methanol synthesis. The methanol steam reforming is considered to be the most favorable process of hydrogen production in comparison to the decomposition and partial oxidation of methanol. This is because of the ability to produce gas with high hydrogen concentration (75%) and high selectivity for carbon dioxide. methanol steam reforming is an endothermic reaction.

3.3.2 Condition of methanol steam reforming

The general reaction conditions of methanol steam reforming are as follows:

· Reaction temperature: 250-375°C

· Pressure: 1 bar

· 1:1 to 1:3 molar ratio of methanol to water

The main products of methanol steam reforming are hydrogen, carbon dioxide and a low content of carbon monoxide. The reaction schemes for the formation of carbon monoxide in methanol steam reforming are shown in Fig 3.3

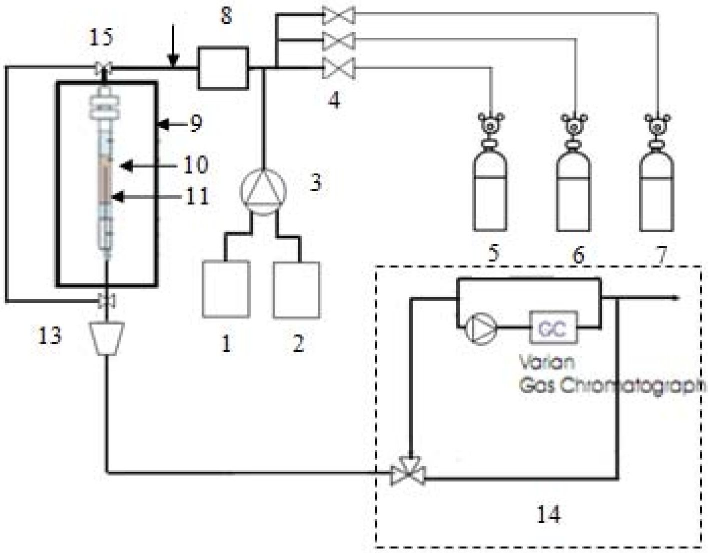

1	MeOH	8	Mixer
2	DI water	9	Furnace
3	HPLC pump	10	Catalyst Bed
4	On-Off Value	11	Thermocouple
5	Dimethyl Ether (DME)	12	Heating Tape
6	Nitrogen (N_2)	13	Water trap
7	Hydrogen (H_2)	14	GC-TCD system
		15	3-ways Valve

Figure 3.3 Schematic diagram of the reaction line for testing the methanol steam reforming by GC-TCD equipped with Poraplot U column and molecular sieve 5 *Å* column.

3.3.3 Mechanisms of methanol steam reforming

There have been some controversies in the literature concerning the mechanisms for production of hydrogen and carbon dioxide by methanol steam reforming. The study of the mechanism of the formation of CO as a by-product has received a high attention. There are several schemes suggested in the literature.

1. No formation of CO in the reaction route. Some researchers suggested the methanol steam reforming process via methyl formate formation, in which no CO takes part in the reaction.

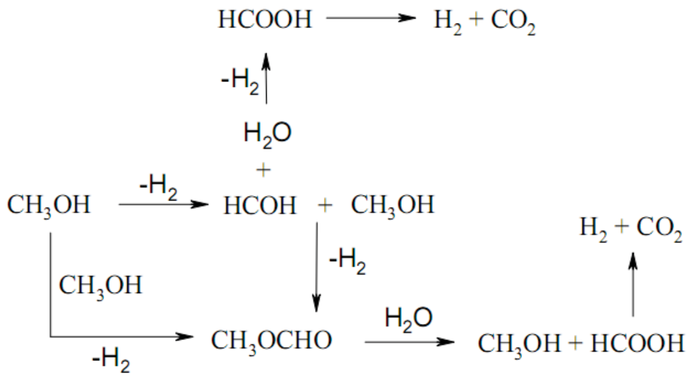

Figure 3.4 mechanism of No formation of CO in the reaction route

2. The decomposition of methanol and water gas shift reaction

$CH_3OH \rightarrow 2H_2O + CO$ (3.5)

$CO + H_2O \rightarrow H_2 + CO_2$ (3.6)

They found that CO concentration was negligible in the product. Based on this result they assumed that CO is produced from decomposition of methanol and followed by water gas-shift reaction, where the decomposition reaction was found to be the rate-determining step. According to this scheme, CO is an intermediate product.

3. The steam reforming of methanol and decomposition of methanol

$$CH_3OH + H_2O \rightarrow 3H_2 + CO_2 \tag{3.7}$$

$$CH_3OH \rightarrow 2H_2O + CO \tag{3.8}$$

A semi-empirical model of the kinetics of the catalyst steam reforming of methanol over $CuO/ZnO/Al_2O_3$ catalyst has been developed by using the reaction schemes of irreversible reaction of methanol steam reforming and decomposition reaction. They found that the water gas-shift reaction could be neglected without substantial loss in accuracy. The rate equations for both reactions can be written as:

$$r_{CH_3OH} = -k_1 C_{CH_3OH} - k_2 \tag{3.9}$$

$$r_{CH_3OH} = -k_1 C_{CH_3OH} \tag{3.10}$$

$$r_{CO_3} = k_1 C_{CH_3OH} \tag{3.11}$$

$$r_{CO} = k_2 \tag{3.12}$$

$$r_{H_2} = 3k_1 C_{CH_3OH} + 2k_2 \tag{3.13}$$

The reaction rate of methanol and water consumption is depending only on the concentration of methanol and not on water concentration. Furthermore, the reaction rate of CO formation is a zero-order rate which means that the formation of CO is not affected by the concentration of methanol or the concentration of water.

4. The steam reforming of methanol, decomposition of methanol and water gas-shift reaction

$$CH_3OH + H_2O \rightarrow 3H_2 + CO_2 \tag{3.14}$$

$$CH_3OH \rightarrow 2H_2O + CO \tag{3.15}$$

$$CO + H_2O \rightarrow H_2 + CO_2 \tag{3.16}$$

The scheme of methanol steam reforming process which includes methanol steam reforming, WGS and decomposition is proposed by Peppley et al. [16]. They studied the reaction network for methanol steam reforming over a Cu/ZnO/Al2O3 catalyst. They claim that in order to fully understand the reaction network, all three reactions must be included in the model. They found that there are two types of catalyst sites that are responsible for the catalyst activity and selectivity, one for the methanol steam reforming and WGS reactions and another for the decomposition reaction.

5. Steam reforming of methanol and reverse water gas shift reaction

The experimental results of CO partial pressure as a function of contact time at different temperatures show very clearly that CO was formed as a consecutive product. The reaction scheme used is the direct formation of CO_2 and hydrogen by SR reaction and formation of CO as consecutive product by reverse WGS reaction. They observed that CO is formed at high methanol conversions and long contact times. No CO was formed at all at low contact times. This indicates that CO is a secondary product, formed by reverse WGS reaction.

$$CH_3OH + H_2O \rightarrow 3H_2 + CO_2 \qquad (3.17)$$

$$H_2 + CO_2 \rightarrow H_2O + CO \qquad (3.18)$$

CHAPTER IV

EXPERIMENTS

This chapter describes the experimental procedure used in this research which can be divided into three sections. The first part explains catalyst preparation by flame spray pyrolysis. The second part shows the details of characterization techniques containing X-ray diffraction (XRD), N_2 physisorption, transmission electron microscopy (TEM), and temperature programmed reduction (TPR). Finally, a detailed procedure for catalyst evaluation in methanol steam reforming is explained.

4.1 Catalyst Preparation

4.1.1 Materials

The chemicals used in the catalyst preparation are all analytical grades as listed in table 4.1. It is noted that specification of these chemicals about physical properties is exhibited later in Appendix A.

Table 4.1 Chemical used for synthesis copper spinel

Chemical	Formula	Grade	Supplier
Ferric actetylacetonate	$C_{15}H_{21}FeO_6$	97%	Sigma-Aldrich
Copper nitrate	$Cu(NO_3)_2 \cdot 2.5H_2O$	98%	Sigma-Aldrich
Ferric nitrate	$Fe(NO_3)_3 \cdot 9H_2O$	98%	Sigma-Aldrich
Manganese nitrate	$Mg(NO_3)_2 \cdot 6H_2O$	98%	
Ethanol	C_2H_5OH	99.9%	JT BAKER

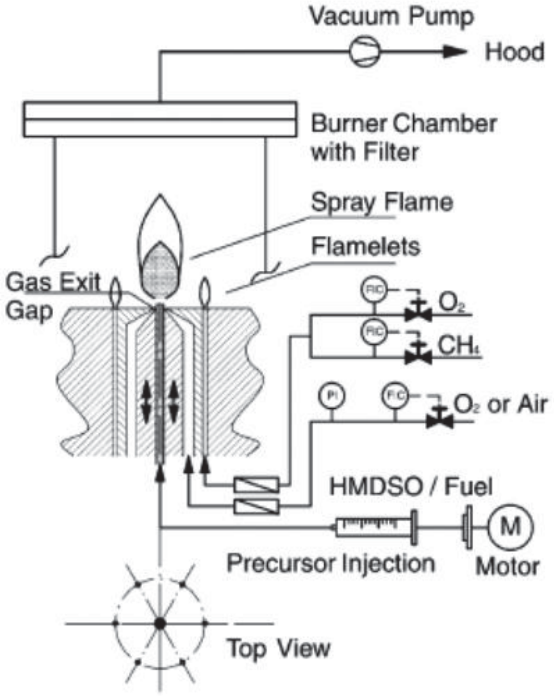

Figure 4.1 Experimental set-up scheme of flame spray pyrolysis [28].

4.1.2 Preparation of copper spinel by Flame Spray Pyrolysis

The flame spray pyrolysis technique was used for preparation of copper spinel catalysts. Copper nitrate ($Cu(NO_3)_2{\cdot}2.5H_2O$), ferric nitrate ($Fe(NO_3)_3{\cdot}9H_2O$) or ferric actetylacetonate ($C_{15}H_{21}FeO_6$) and manganese nitrate ($Mg(NO_3)_2{\cdot}6H_2O$) were used as precursors, which was diluted with ethanol to a 0.3 M solution. The mixed precusors was injected through the center capillary of the flame spray pyrolysis nozzle by a syringe pump at 5 ml/min. Oxygen was fed at 5 l/min through the surrounding annulus dispersing the solution into droplets. The pressure drop at the nozzle was held constant at 1.5 bar by adjusting the annulus gap width. A supporting premixed CH_4/O_2 surrounded by the dispersion oxygen annulus ignited and stabilized the spray flame. A sinter metal ring surrounding the CH_4/O_2 flame was supplied by additional 5 l/min O_2-sheath. The equipment of flame spray pyrolysis is shown in figure 4.1. To accommodate for discussion, the catalysts used in this research are symbolically assigned as shown in Table 4.2.

Table 4.2 The symbol of the catalysts prepared using the different conditions

catalysts	Precursor	Symbol
Effect of precursor		
1:2$CuFe_2O_4$ 0.3M Flow 5	Ferric actetylacetonate + Copper nitrate	Cu1Fe2_mix
	Ferric nitrate + Copper nitrate	Cu1Fe2_NO
Effect of concentration		
1:2$CuFe_2O_4$ 0.1M Flow 5	Ferric nitrate +	5Cu1Fe2-0.1M
1:2$CuFe_2O_4$ 0.3M Flow 5	Copper nitrate	5Cu1Fe2-0.3M
1:2$CuFe_2O_4$ 0.5M Flow 5		5Cu1Fe2-0.5M
Effect of flow		
1:2$CuFe_2O_4$ 0.3M Flow 3	Ferric nitrate +	3Cu1Fe2-0.3M
1:2$CuFe_2O_4$ 0.3M Flow 5	Copper nitrate	5Cu1Fe2-0.3M
1:2$CuFe_2O_4$ 0.3M Flow 7		7Cu1Fe2-0.3M
Effect of ratio of Copper and Ferric		
1:4$CuFe_2O_4$ 0.3M Flow 5	Ferric nitrate +	Cu1Fe3
1:2$CuFe_2O_4$ 0.3M Flow 5	Copper nitrate	Cu1Fe2
1:1$CuFe_2O_4$ 0.3M Flow 5		Cu1Fe1
Effect of metal composition		
$CuFe_2O_4$ 0.3M Flow 5	Ferric nitrate +	Cu1Fe2
$CuFe_{1.5}Mn_{0.5}O_4$ 0.3M Flow 5	Copper nitrate+	Cu1Fe1.5Mn0.5
$CuFeMnO_4$ 0.3M Flow 5	Manganese nitrate	Cu1Fe1Mn1
$CuFe_{0.5}Mn_{1.5}O_4$ 0.3M Flow 5		Cu1Fe0.5Mn1.5
$CuMn_2O_4$ 0.3M Flow 5		Cu1Mn2

4.2 Catalyst Characterization

4.2.1 X-ray Diffraction (XRD)

The X-ray diffraction patterns of powder were obtained using an X-ray diffractometer BRUKER D8 ADVANCE connected with a computer with Diffract Plus TROPAS 4.2 programmed for fully control of the XRD analyzer. The experiments were carried out using Ni-filtered CuKα radiation. Scans were performed over the 2θ ranges from 20° to 80°. The crystallite size was estimated from line broadening according to the Scherrer equation. This instrument has been located at National Nanotechnology Center (NANOTEC), National Science and Technology Development Agency (NSTDA).

4.2.2 N_2 Physisorption

The BET surface areas for the multipoint method were measured by N_2 physisorption using BEL SORP mini II. The catalysts were firstly pretreated in 50 ml/min of helium gas flow at 150 °C for 3 h. Sample pretreatment system was used to remove water bound to the particle surface from air moisture. After cooled down to the ambient temperature, the weight of dried catalyst was collected. Sample cell was installed to the adsorption part. The requisite data were input to the software before the measurement. The sample cell was dipped in the dewar containing liquid nitrogen. The volume of N_2 was measured at -196 °C using the different N_2 partial pressure and then the adsorption-desorption isotherm was plotted.

4.2.3 Transmission Electron Microscopy

The sizes and shapes of the samples were observed by a transmission electron microscope (JEOL, JEM-2010) operated at 200 kV. This instrument has been located at National Metal and Materials Technology Center, National Science and Technology Development Agency (NSTDA), Thailand. The sample was dispersed in ethanol to obtain the uniform dispersion of sample. A drop of liquid was deposited onto a copper mesh sample grid that supported a holey carbon support film. The grid was resting on a filter paper and was allowed to dry for several minutes before being moved. The scans were done many times in different areas as much as possible until the good representative image for all areas was obtained.

4.2.4 Temperature Programmed Reduction

Temperature programmed reduction was used to determine the reducibility of catalysts. The hydrogen consumption was measured by using a Micrometritics Pulse Chemisorb 2750 instrument at National Metal and Materials Technology Center, National Science and Technology Development Agency (NSTDA), Thailand. 10% H_2 in Ar and N_2 in ultra-high purity grade were used as a probe molecule gas and a carrier gas, respectively. 0.1 g of a catalyst sample was placed in a quartz tubular reactor. Under N2 atmosphere at a flow rate of 25 ml/min, the catalyst sample was heated up to 250 °C at a heating rate of 10 °C/min and held for 1 h at this temperature in order to eliminate the adsorbed water. After the pretreatment, the system was cooled down to room temperature. The reduction step was performed under 10% H_2 in Ar flow of 25 ml/min from room temperature to 800 °C at a heating.

4.3 Catalyst Evaluation

Catalytic activity of all samples in methanol steam reforming was evaluated in a conventional flow reactor under atmospheric pressure. The gases used in catalytic activity and product selectivity test are listed in Table 4.3. They were all supplied by Thai Industrial Gas Limited.

Table 4.3 The details of gases used in the catalyst activity test activity product selectivity.

Gases	Formula	Grade
Nitrogen	N_2	99.999%
Dimethyl Ether	CH_3OCH_3	-
Hydrogen	H_2	99.999%

The apparatus consisted of a fixed-bed reactor, an electrical furnace, an automation temperature controller, a gas controlling system, and online gas chromatographs equipped with a thermal conductivity detector. Catalytic activity measurements were carried out in a fixed bed stainless steel tubular reactor (0.95 cm. inside diameter). The catalyst sample was placed between two quartz wool layers. . The gas flows were adjusted by the metering valves. The electrical furnace was used to supply heat to the reactor. The reactor could be operated from room temperature up to 800 °C at the maximum voltage of 220 V. Reactor temperature was measured at the bottom of the catalyst bed in the reactor by automation temperature controller (Figure 3.3).

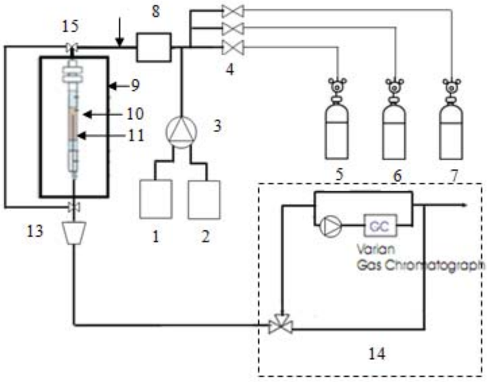

8	MeOH	8	Mixer
9	DI water	9	Furnace
10	HPLC pump	10	Catalyst Bed
11	On-Off Value	11	Thermocouple
12	Dimethyl Ether (DME)	12	Heating Tape
13	Nitrogen (N_2)	13	Water trap
14	Hydrogen (H_2)	14	GC-TCD system
		15	3-ways Valve

Figure 3.3 Schematic diagram of the reaction line for testing the methanol steam reforming by GC-TCD equipped with Poraplot U column and molecular sieve 5 Å column.

A catalyst sample (0.2g) was packed in a fixed-bed reactor placed in the furnace. Prior to the evaluation of the catalytic activity, the catalyst was reduced by hydrogen at a designed reduction temperature in range 200-400℃ in nitrogen flow rate of 20 ml/min with a heating rate of 10 °C/min and the catalyst was reduced with flow rate of 40 ml/min for 1 h in 10%H_2/N_2. After the reduction, the reactor was cooled to 200°C in nitrogen flow under atmospheric pressure. A mixture of MeOH and steam at a fixed steam to carbon ratio (S/C) at 2.0 were supplied to a pre-heater at temperature of ca. 150℃, the total volumetric flow rate was 30 ml/min and then to the catalyst bed at designed reaction temperature through mass flow controllers. The reaction temperature was varied in the range 200-375℃. Compositions of influent and effluent gas were analyzed by online gas chromatographs equipped with a thermal conductivity detector (VARIAN, CP-4900) when time to 30 minute. The steam in the feed and reformate was trapped by a condenser at ca. 3 ℃ before the gas analysis. A Poraplot U column was used for separation of dimethyl ether, MeOH, and CO_2, and a molecular sieve 5A column for separation of H_2, O_2, N_2, CH_4, and CO.

Table 4.4 The operating conditions of TCD gas chromatographs for the catalytic activity test

Gas chromatograph	VARIAN, CP-4900	
Column	Poraplot U	molecular sieve 5Å
Carrier gas	Helium	Helium
Carrier gas flow	N_2	N_2
Injector temperature	150	150
Detector temperature	100	100
Column temperature	100	100
Analysis gas	DME, MeOH, and CO_2	H_2, O_2, N_2, CH_4, and CO

CHAPTER V

RESULTS AND DISCUSSION

This chapter presents the results with a discussion about the characteristics and the catalytic properties of copper based spinel catalysts in the methanol steam reforming (MeOH SR) and dimethyl ether steam reforming (DME SR). The reaction temperature was varied in the range 200-375°C under atmospheric pressure. In this work, the preparation condition of the Cu-based spinel catalysts by flame spray pyrolysis (FSP) and compositions of Cu-based spinel catalysts in term of ratio copper and ferrite with in term of manganese loading were investigated to fine tune the optimal condition. Influence of temperature reduction was also studied. Additional, the best of result of prior section were tested in term of dimethyl ether steam reforming. Therefor the results and discussion are divided into four sections. In the first section, the effect of condition preparation of copper based spinel catalysts in flame spray pyrolysis step e.g. the effect of precursor's types, the effect of concentrations of precursors and the effect of precursors feed rates. The next section studied the effect of composition loading for copper based spinel catalysts follow that the effect of temperature reduction of copper based spinel catalysts. Finally, the catalysts evaluation in term of dimethyl ether steam reforming also studied

All of sections were studied the physical and chemical properties of Cu based spinel catalysts e.g. the phase identification was determined by the X-ray diffraction technique (XRD). The morphology and particle characteristics were focused by transmission electron microscopy (TEM). The N_2 physisorption showed the BET surface area. The adsorption/desorption isotherms and the pore size distribution, which were also obtained by the N_2 physisorption, indicated the pore characteristics of the catalysts. The temperature programmed reduction (TPR) exhibited reduction behavior and reducibility of catalysts and the catalysts performance for the methanol steam reforming and dimethyl ether steam reforming are also evaluated**.**

5.1 The effect of condition preparation of copper based spinel catalysts in flame spray pyrolysis step

In this past, studied condition of copper based spinel catalysts in flame spray pyrolysis step by distribute three conditions, the effect of precursor's types of copper based spinel catalysts in flame spray pyrolysis step by varied precursors, copper nitrate mixed with ferrite nitrate (NO) as precursor was saluted in ethanol and copper nitrate mix with ferrite acetylacetonate (MIX) as precursor was also soluted in ethanol were investigated. Next, studied effects of concentration precursor of copper based spinel catalysts in flame spray pyrolysis step. The concentration of precursor was varied in the range 0.1-0.3M. Finally, also studied effects of precursor feed rate in flame spray pyrolysis step by varied in the range 3-7 ml/min.

5.1.1 The Physical and Chemical Properties of copper based spinel catalysts

- **The BET Surface Area and Pore Characteristics**

The table 5.1 show BET surface area and particle diameter of copper based spinel catalysts by flame spray pyrolysis in term of effect of precursor's types. Results show that, copper based spinel Cu1Fe2_MIX have particle smaller than CuFe2_NO. Additional, BET surface area and the particle diameter of each of conditions of copper spinel catalysts by flame spray pyrolysis such as effects of concentration precursor and effects of precursor feed rate expressed that increasing concentration from 0.1M-0.3M and increasing the precursor feed rate from 3 to 7 ml/min, decreased the surface area from 100 to 63 m^2/g and decreased from 71 to 51 m^2/g, respectively. Because increasing the precursor concentration through the liquid feed rate continuously increases the product primary particle diameter as the particle concentration and residence time at high temperatures increase. The spray flame temperature is high enough for the primary particles of the aggregates to coalesce to solid particles[29]. This indicates that particle formation takes place in the gas phase results in solid nano-sized particles and not hollow ones which can also be formed during or flame spray pyrolysis[30]. Moreover, calculation from TEM and BET surface area mean have equal particle by calculation from TEM based on from figure 5.4-5.8 and calculation from BET surface area based on from table 5.1.

Table 5.1 The BET surface area and the particle diameter Cu based spinel catalysts.

Catalysts	**Condition**	**BET surface area (m^2/g)**	**Particle diameter[a] (nm)**	**Particle diameter[b] (nm)**
Effect of precursor				
Cu1Fe2_mix	MIX	70	-	10
Cu1Fe2_NO	NO	63	7	11
Effect of concetration				
5-Cu1Fe2-0.1M	NO	100	6	7
5-Cu1Fe2-0.3M	NO	63	7	11
5-Cu1Fe2-0.5M	NO	41	12	18
Effect of precursor feed rate				
3-Cu1Fe2-0.3M	NO	71	8	10
5-Cu1Fe2-0.3M	NO	63	7	11
7-Cu1Fe2-0.3M	NO	51	14	14

[a] Based on transmission electron microscopy.

[b] Based on BET surface area Mean: Particle diameter (nm) = 6/(density × S_{BET})

- **The Phase Analysis by X-ray Diffraction**

The X-ray diffraction pattern of copper ferrite spinel catalysts prepared by flame spray pyrolysis in each precursor is shown in figure 5.1. The XRD peaks at 18°, 30°, 33°, 35°, 37°, 43°, 53°, 57° and 62° were evident for the both of copper ferrite spinel catalysts in the cubic phase [12]. Spinel structures have been made by flame spray pyrolysis because the metal precursors evaporate in this spray flame and are combusted. The process features short residence times (a few milliseconds) and high maximum process temperatures (up to 3000K) [1]. However, crystallize size of both copper ferrite spinel catalysts have two times the size different by copper ferrite spinel (NO) is larger than ones. The crystallize size can based on Scherrer equation is shown in table 5.2.

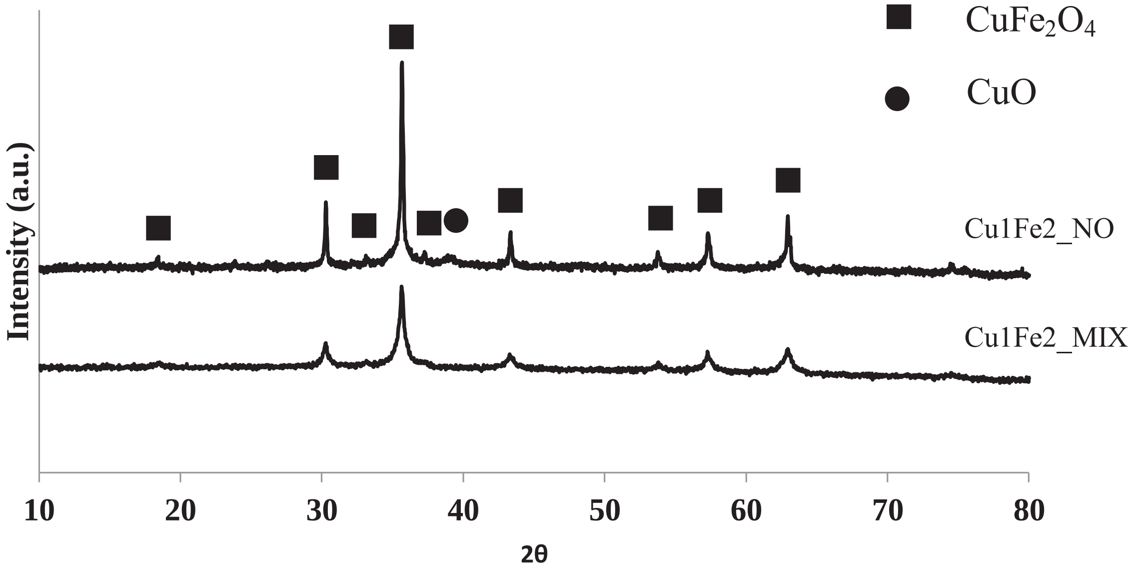

Figure 5.1 XRD patterns of effect of precursor types in flame spary pylolysis preparation step.

Figure 5.2-5.3 shows X-ray diffraction pattern of copper ferrite spinel catalysts of effect precursor concentration and precursor feed rate. Result shows that, increasing precursor concentration as well as feed flow rate would increase particle size and higher of flame due to increase feed flow rate increase the time for fuel combustion and also increase particle size[31]. The d_{XRD} for copper ferrite spinel catalysts 5Cu1Fe2_0.1M, 5Cu1Fe2_0.3M and 5Cu1Fe2_0.5M were determined to be 26, 38 and 50 nm, respectively. Additional, The d_{XRD} for copper ferrite spinel catalysts 3Cu1Fe2_0.3M, 5Cu1Fe2_0.3M and 7Cu1Fe2_0.3M were determined to be 25, 38 and 40 nm, respectively. It is indicated that the crystallinity of flame spray pyrolysis - made catalysts increased as higher of flame and also longer resident time.

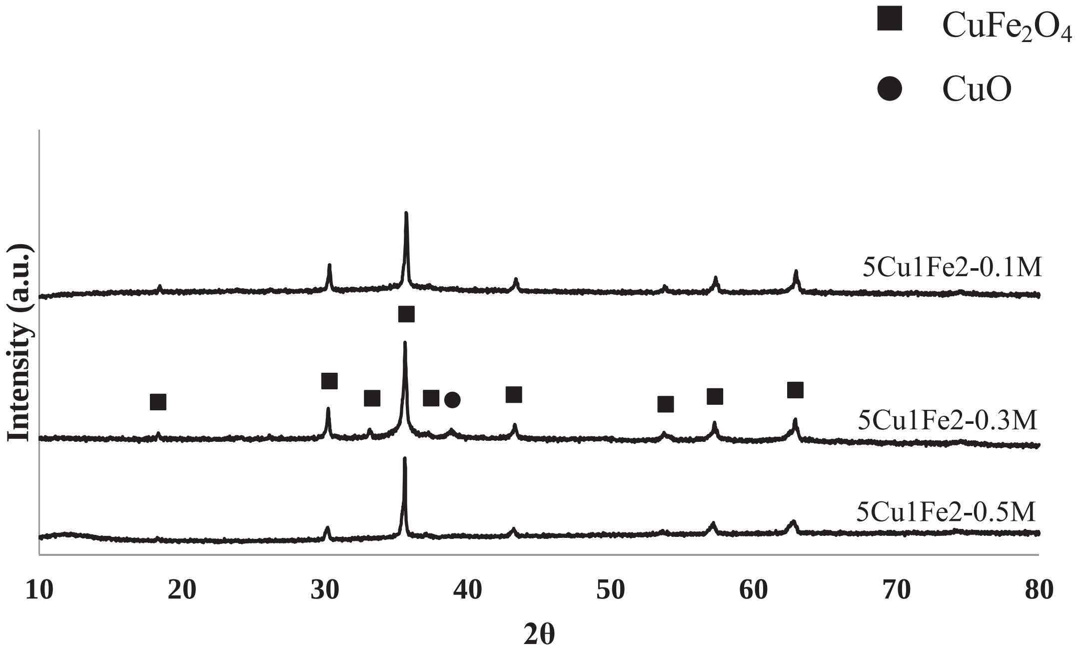

Figure 5.2 XRD pattern of effect of concentration of precursor in flame spary pylolysis preparation step.

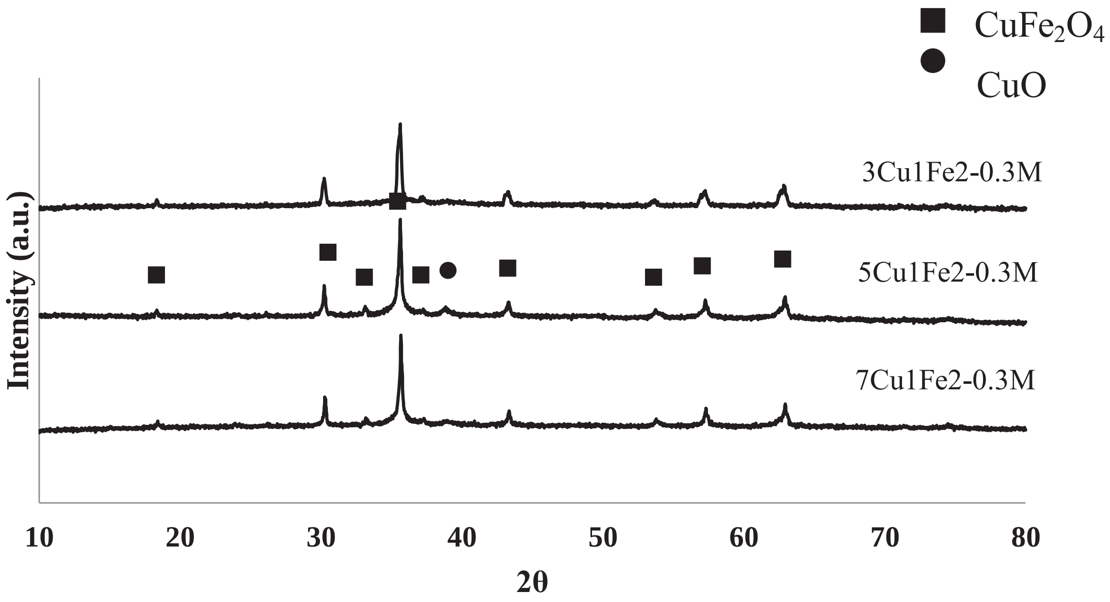

Figure 5.3 XRD pattern of effect of precurcur feed rate in flame spary pylolysis preparation step.

Table 5.2 Particle diameter from BET, average particle diameter from TEM and Crystallize size of Cu based spinel catalysts.

Catalysts	**Particle diameter[a] (nm)**	**Particle diameter[b] (nm)**	**Crystallize size[c] (nm)**
Effect of precursor			
Cu1Fe2_mix	-	-	18
Cu1Fe2_NO	7	12	38
Effect of concetration			
5Cu1Fe2-0.1M	6	7	26
5Cu1Fe2-0.3M	7	12	38
5Cu1Fe2-0.5M	12	18	50
Effect of precursor feed rate			
3Cu1Fe2-0.3M	8	10	25
5Cu1Fe2-0.3M	7	12	38
7Cu1Fe2-0.3M	14	14	40

[a]Based on transmission electron microscopy.
[b]Based on BET surface area Mean: Particle diameter (nm) = 6/(density × S_{BET})
[c]Based on Scherrer equation

- **Transmission Electron Microscopy (TEM)**

In order to determine the particle morphology and the particle size distribution, a powerful technique such as TEM was applied to samples. TEM micrographs of copper spinel catalysts of this section are shown in figures 5.4-5.8. The shape of catalysts particles was rather spherical and non-hollow with an average size in range 6-14 nm because effect from increased precursor concentration and precuesor feed rate. The particle sizes of each catalysts prepared by flame spray pyrolysis were varied because it was difficult to control particle formation during the flame spray process. But maybe control particle formation when precursor have optimal condition such as precursor concentration, precursor feed rate and oxygen dispersion. Suggest that, increasing precursor concentration and precursor feed rate, increased difficult to control particle formation during the flame spray process when investigated from figures 5.4-5.8.

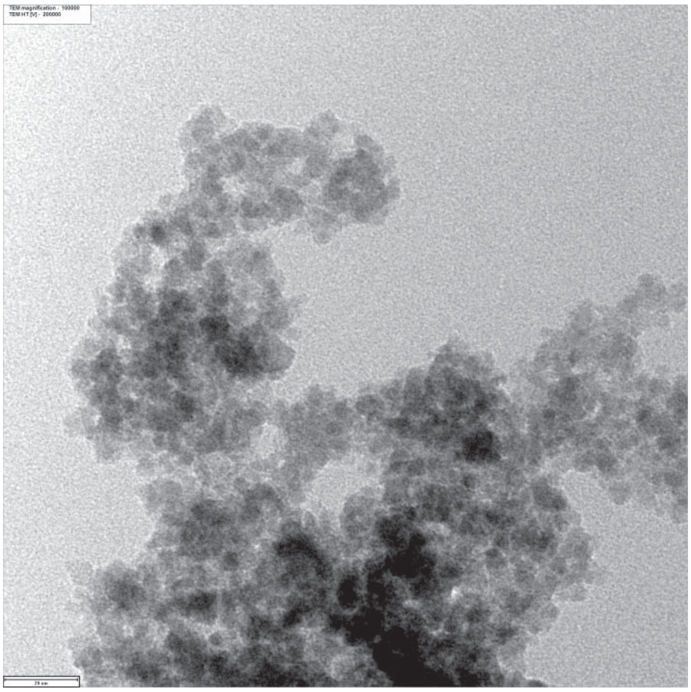

Figure 5.4 Transmission electron microscopy image of 5Cu1Fe2-0.1M catalyst**.**

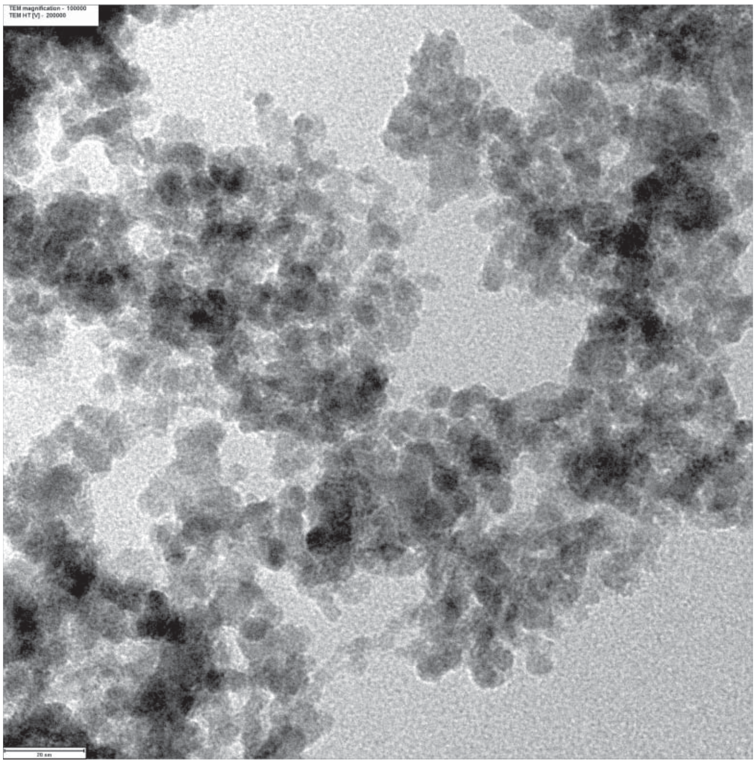

Figure 5.5 Transmission electron microscopy image of 5Cu1Fe2-0.3M catalyst**.**

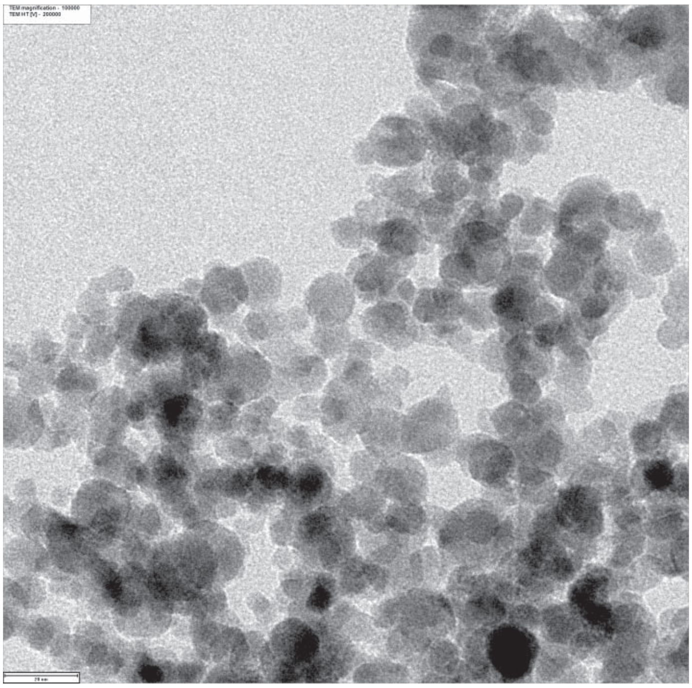

Figure 5.6 Transmission electron microscopy image of 5Cu1Fe2-0.5M catalyst.

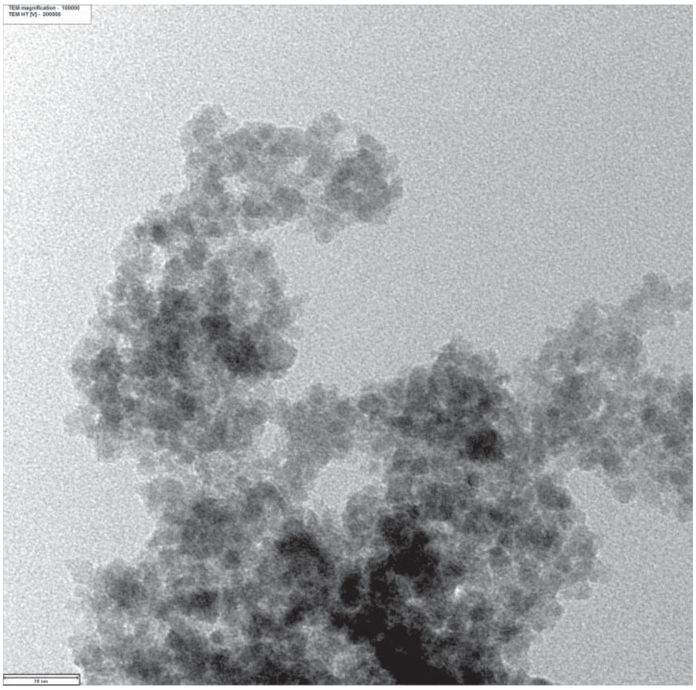

Figure 5.7 Transmission electron microscopy image of 3Cu1Fe2-0.3M catalyst.

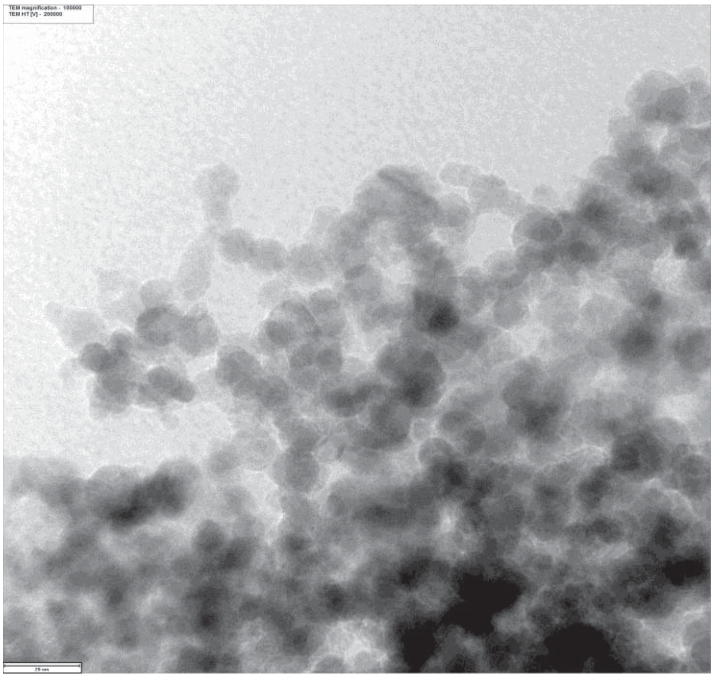

Figure 5.8 Transmission electron microscopy image of 7Cu1Fe2-0.3M catalyst.

- **The temperature programmed reduction**

Temperature programmed reduction was performed in order to determine the reduction behaviors. Figure 5.9-5.11 shows TPR profile of copper ferrite spinel catalysts of each condition. Normally, copper ferrite spinel show two main reduction peaks, Fe_2O_3 to Fe_3O_4 around 200-300°C and Fe_3O_4 to Fe^0 around 260°C and 450°C, respectively[11] and one shoulder peak was $CuFe_2O_4$ to Cu^0 and Fe_2O_3 around 200°C. For effect of precursor types shows that Cu1Fe2_NO have reduction behavior similar with mentioned above while Cu1Fe2_MIX consis of three main peaks suggest that when $CuFe_2O_4$ was reduced to Cu^0 and Fe_2O_3. However, the Fe_2O_3 not changed immediately into Fe_3O_4. Additional the Cu1Fe2_NO completely reduced faster than Cu1Fe2_MIX (Figure 5.9). For effect of concentration of precursor and precursor feed rate (figure 5.10), 5Cu1Fe2 0.5M was shifted to a higher temperature and the peak reduction of $CuFe_2O_4$ to Cu^0 which easier reduction than other catalysts because used small hydrogen consumption. However the 5Cu1Fe2-0.3M and 7Cu1Fe2-0.3M used very high hydrogen consumption to changed Fe_2O_3 into Fe_3O_4 while 3Cu1Fe2-0.3M and 5Cu1Fe2.0.1M used high hydrogen consumption smaller than ones because decreased particle size of catalysts would low interaction between molecules catalysts so thay easier reduction.

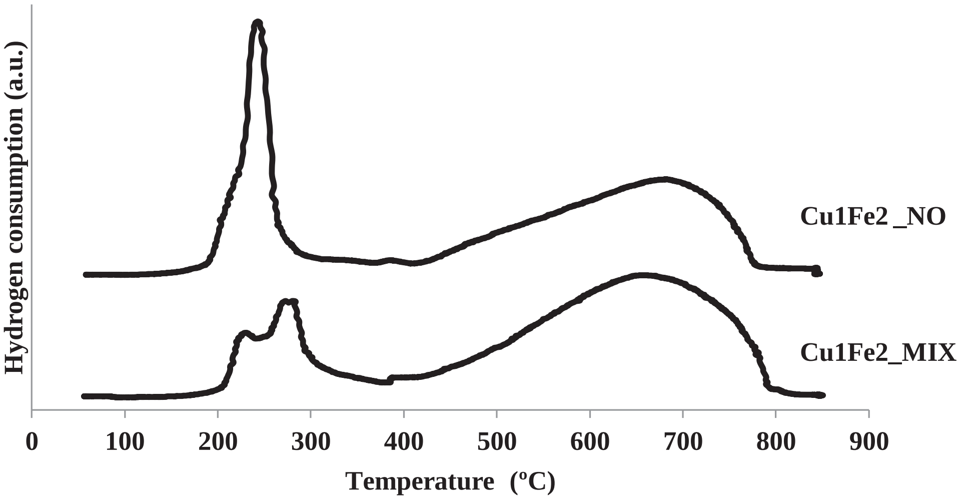

Figure 5.9 TPR profiles of effect of precursor types in flame spary pylolysis preparation step

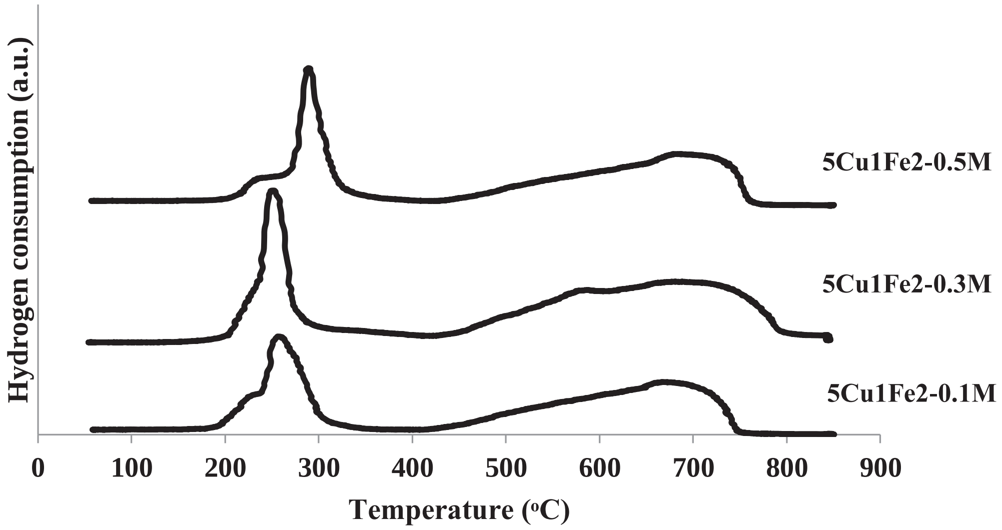

Figure 5.10 TPR profiles of effect of precursor concentration in flame spary pylolysis preparation

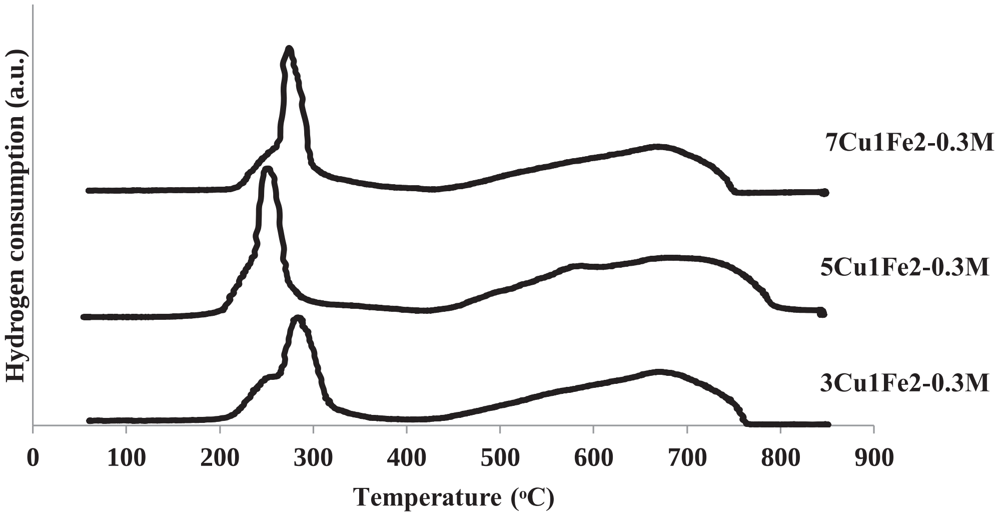

Figure 5.11 TPR profile of effect of precursor feed rate in flame spary pylolysis preparation.

5.1.2 Catalytic evaluated performance for the methanol steam reforming

Figure 5.12-5.13 shows methanol conversion and hydrogen production rate and CO selectivity of catalysts in this section. The copper ferrite spinel catalysts commercial was used reference of effect of condition catalysts. The effect of precursor types shows that, Cu1Fe2_NO provided superior catalytic activity and hydrogen production rate than Cu1Fe2_MIX and copper ferrite commercial catalyst. The reasonable of this results can described the Cu1Fe2_NO easier reduction than Cu1Fe2_MIX and after complete reduction, the active spinel structure of Cu1Fe2_NO better performance for methanol steam reforming reaction than the active spinel structure of Cu1Fe2_MIX.

Moreover, in case of each condition such as effect of precursor concentration and precursor feed rate show that increasing precursor concentration and precursor feed rate, increased catalytic activity and hydrogen production except the 7Cu1Fe2-0.3M. Especially, the 5Cu1Fe2-0.5M provided superior catalytic activity, hydrogen production and CO selectivity in methanol steam reforming because the 5Cu1Fe2-

0.5M has the easiest reduction and the largest particle size which would rich Cu^0 but influence of the large particle size of catalysts through its effect intraparticle diffusion limitations maybe increased CO concentration. However the 5Cu1Fe2-0.3M not provided superior catalytic activity and hydrogen production rate but provided the smallest CO selectivity. For this section studied optimal condition of catalysts for studied in next section which the 5Cu1Fe2-0.3M was the optimal catalyst condition.

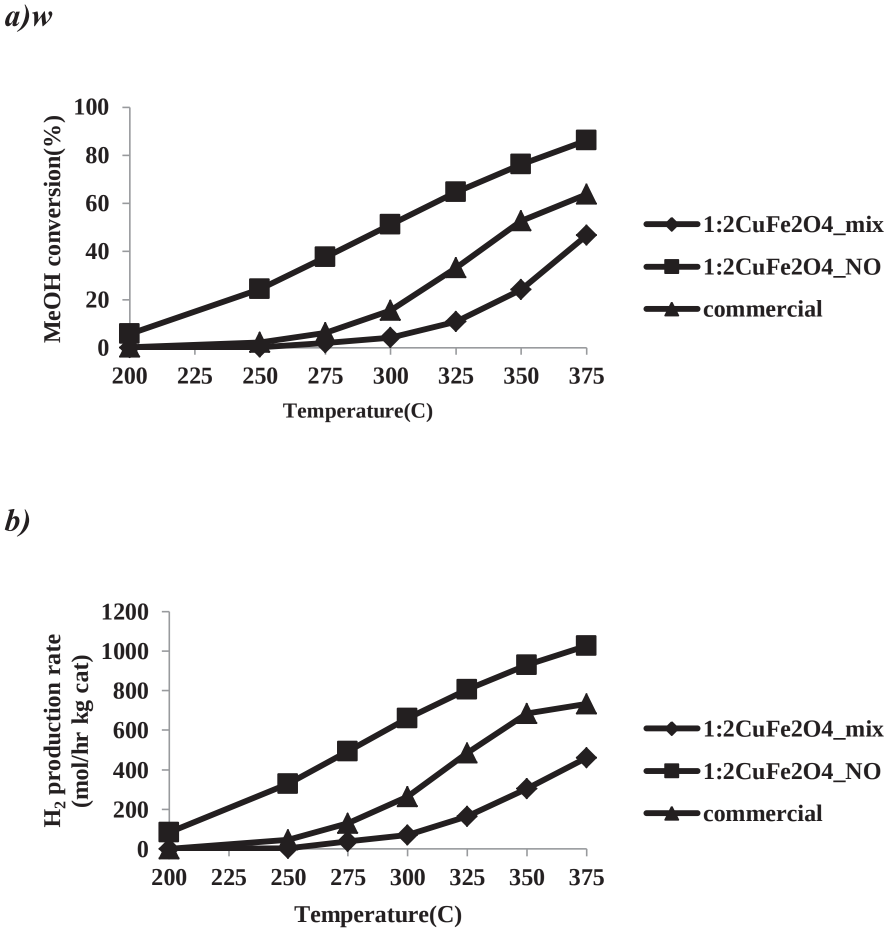

Figure 5.12 Effect of precursor type on a) MeOH conversion and b) hydrogen production rate over copper spinel in methanol steam reforming..

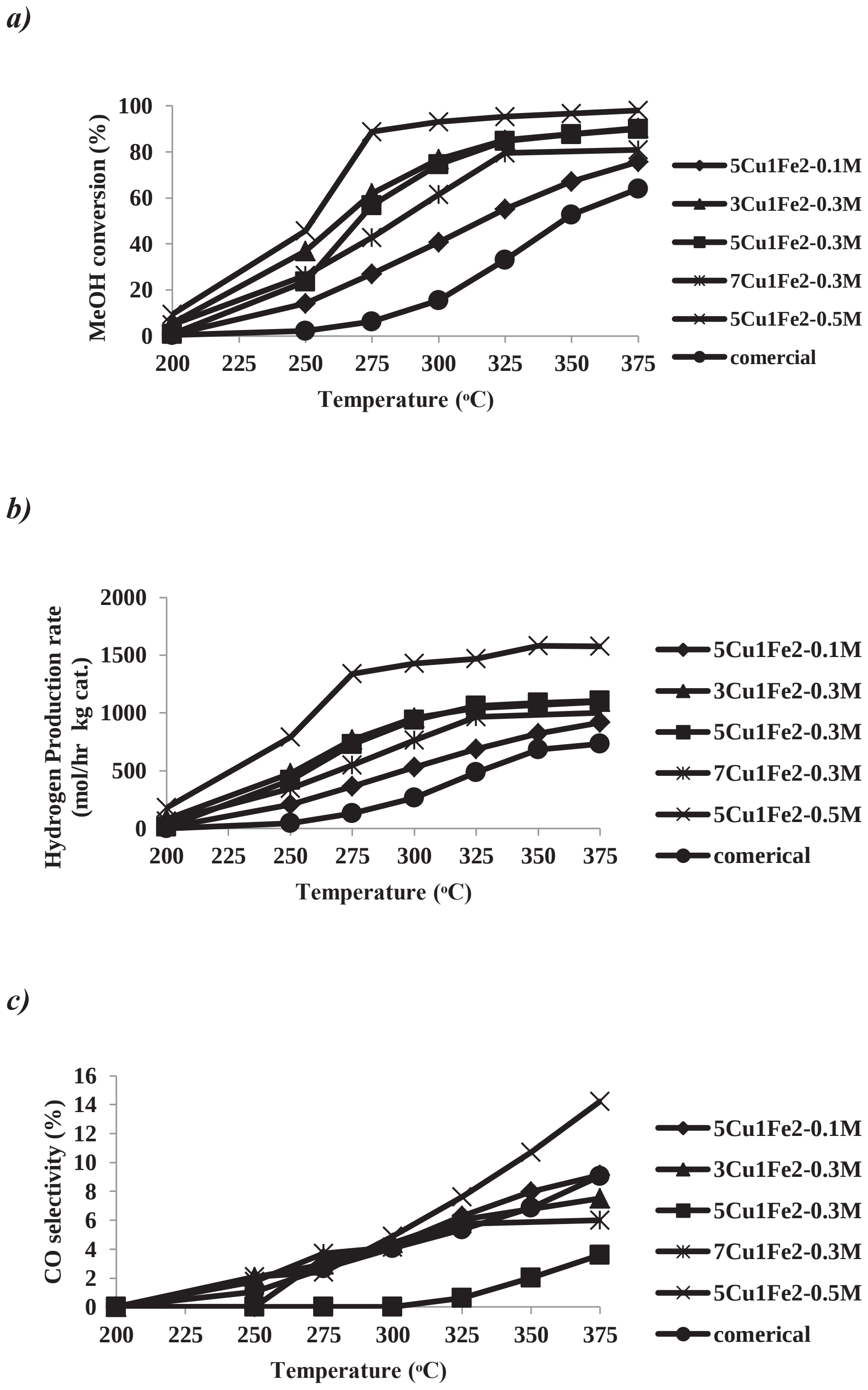

Figure 5.13 Effect of precursor feed rate and precursor concentration on a) MeOH conversion b) hydrogen production rate and c) CO selectivity over copper spinel in methanol steam reforming.

5.2 The effect of composition loading of copper based spinel catalysts

In this past, studied effect of composition loading of copper based spinel catalysts in flame spray pyrolysis step by distribute two conditions, effect of copper and ferrite ratio in flame spray pyrolysis step. The ratio of copper and ferrite was varied Cu1Fe3, Cu1Fe2 and Cu1Fe1 by chosen optimal condition of ratio tetrahedral size and octahedral size. Next step studied the effect of manganese loading in flame spray pyrolysis step was investigated. The ratio of copper spinel was fixed tetrahedral site as 1 and varied octahedral site as Cu1Fe2, Cu1Fe1.5Mn0.5, Cu1Fe1Mn1, Cu1Fe0.5Mn1.5, and Cu1Mn2.

5.2.1 The effect of copper and ferrite ratio.

The Physical and Chemical Properties of copper based spinel catalysts

- **The Phase Analysis by X-ray Diffraction**

Figture 5.14 studied effect of copper and ferrite ratio in precursor was prepared by flame spray pyrolysis step. The fresh catalysts were varied 1:3, 1:2, and 1:1. Result shows that, all samples have spinel structure by investigated XRD peaks at 18°, 30°, 33°, 35°, 37°, 43°, 53°, 57° and 62° [12], The intensity of XRD peak of the CuO ($2\theta = 39°$) phase increased with copper content which Cu1Fe1 consist of copper 50%, it have the highest intensity of XRD peak of the CuO. However the Cu1Fe3 catalysts have the smallest copper content (25%copper loading), the intensity of XRD peak of the CuO have the smallest.

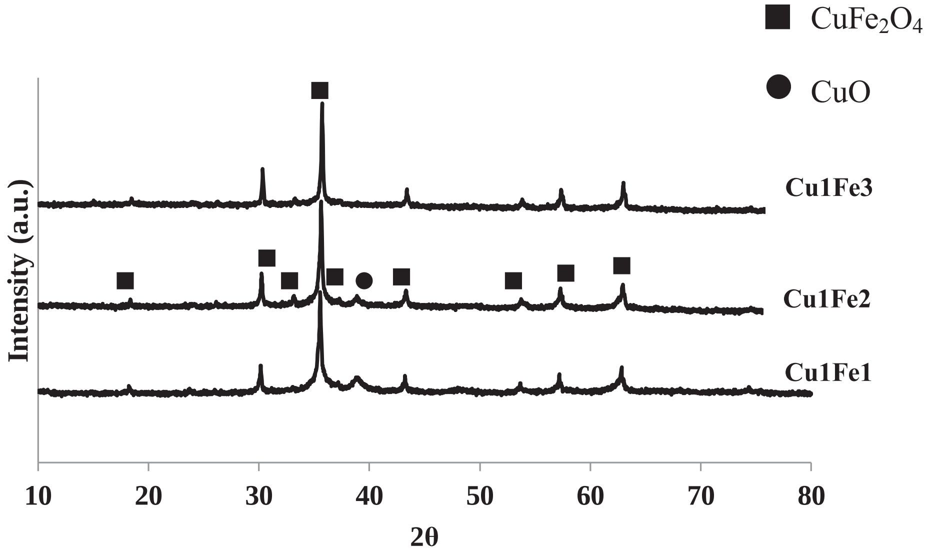

Figure 5.14 XRD pattern of effect of copper and ferrite ratio in flame spary pylolysis preparation step.

- **The BET Surface Area**

The specific surface area of copper and ferrite ratio in precursor was prepared by flame spray pyrolysis step were showed in table 5.3. The specific surface areas of the catalysts were 63 m^2/g which all catalysts as well. Therefore, the particles size of catalysts this section not significant for methanol steam reforming.

Table 5.3 The BET surface area of effect of copper and ferrite ratio

Catalysts	BET surface area (m^2/g)
5-Cu1Fe1-0.3M	64
5-Cu1Fe2-0.3M	63
5-Cu1Fe3-0.3M	63

- Transmission Electron Microscopy (TEM)

From figure 5.15-5.17 showed TEM images of copper and ferrite ratio in precursor area of copper and ferrite ratio in precursor was prepared by flame spray pyrolysis step. Results show that, increasing copper loading, increased particle from 7-14 nm. by the catalysts in condition 5-Cu1Fe3-0.3M have the smallest particle size while the catalysts in condition 5-Cu1Fe2-0.3M have the largest particle size. The shape of catalysts in this section was rather spherical and non-hollow.

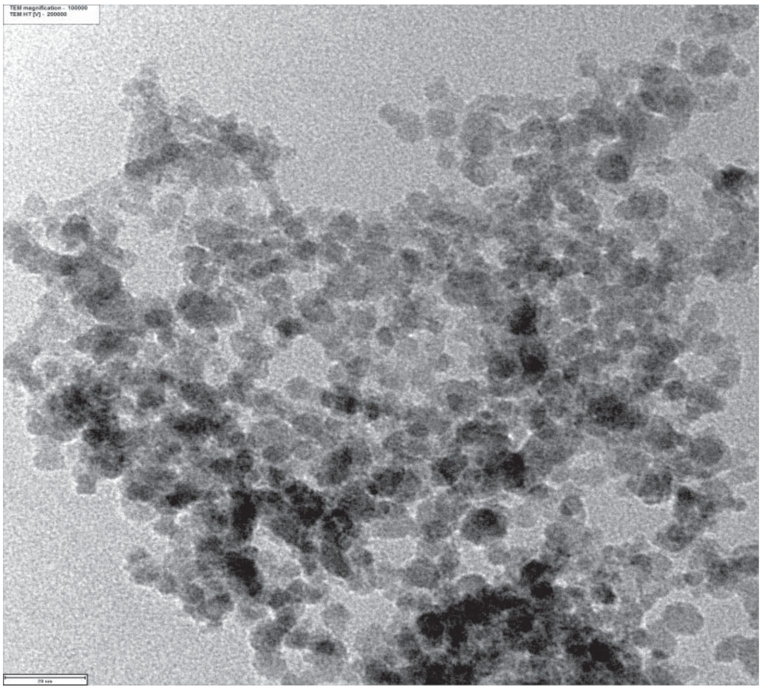

Figure 5.15 Transmission electron microscopy image of 5Cu1Fe3-0.3M catalyst.

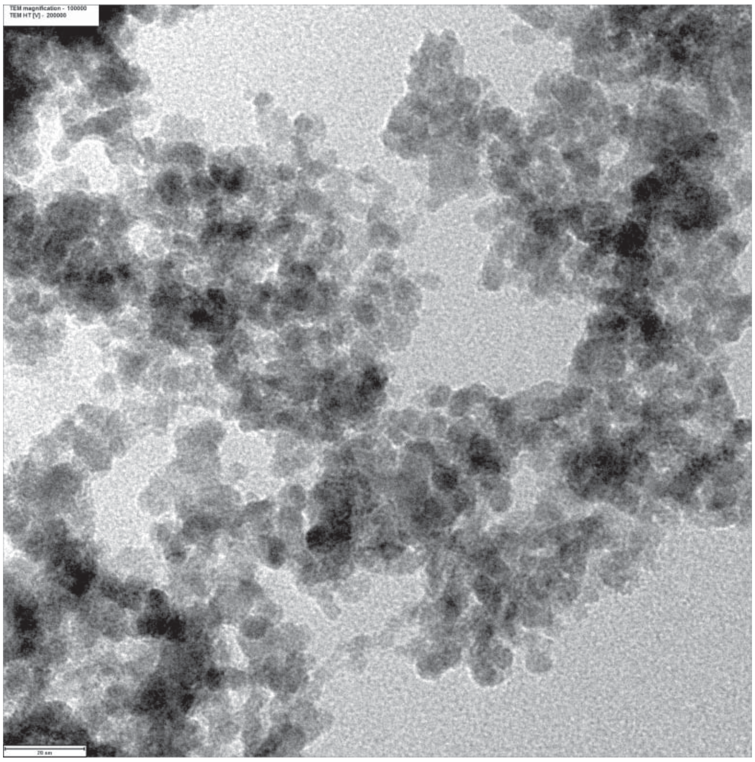

Figure 5.16 Transmission electron microscopy image of 5Cu1Fe2-0.3M catalyst

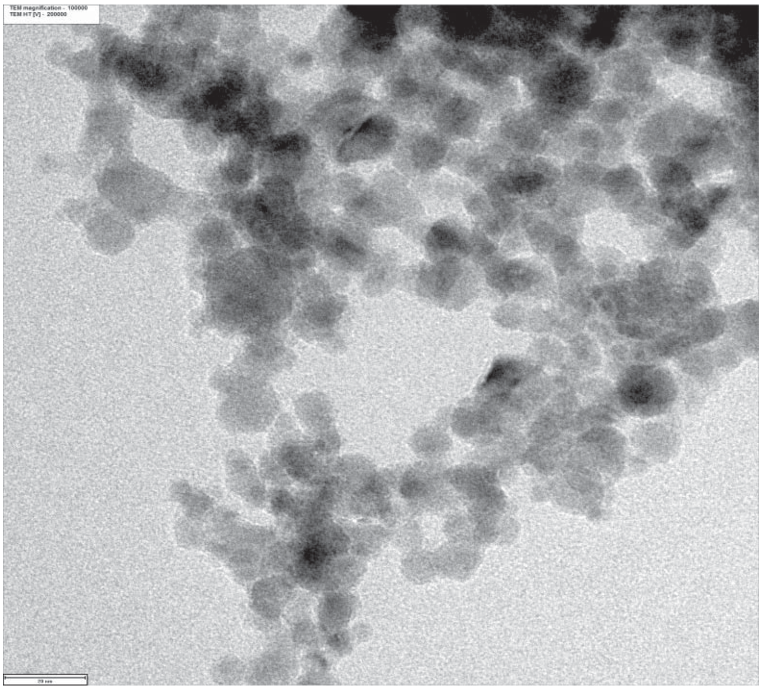

Figure 5.17 Transmission electron microscopy image of 5Cu1Fe1-0.3M catalyst

- **The temperature programmed reduction**

The reducibility of copper and ferrite ratio in precursor area of copper and ferrite ratio in precursor was prepared by flame spray pyrolysis step were investigated by TPR measurement. Figure 5.18 shows TPR profiles of copper spinel of each condition, the $CuFe_2O_4$ in Cu1Fe1 catalyst was reduced from copper spinel to Cu^0 in temperature range 200-280℃ and used the highest hydrogen consumption, indicated that the Cu1Fe1 catalysts consist of copper spinel and copper oxide with the high of copper content. In agreement with previous studies, pure CuO was reduced to metallic copper in a single step and in the temperature range 250-350℃[32]. Additional from previous copper spinel in dimethyl ether steam reforming studied, the copper ferrite spinel show two main reduction peaks, Fe_2O_3 to Fe_3O_4 around 200-300°C and Fe_3O_4 to Fe^0 around 260°C and 450°C, respectively[11] and one shoulder peak was $CuFe_2O_4$ to Cu^0 and Fe_2O_3 around 200°C. Therefore the TPR profile of Cu1Fe1 catalyst has reduction behavior similar between the both catalysts. Furthermore, the Fe_3O_4 reduction of Cu1Fe1 catalyst also the fastest reduce in TPR measurement. Nevertheless the intensity of Cu1Fe3 and Cu1Fe2 catalysts was similar except Cu1Fe1 because effect of copper loading and result from TEM and XRD pattern.

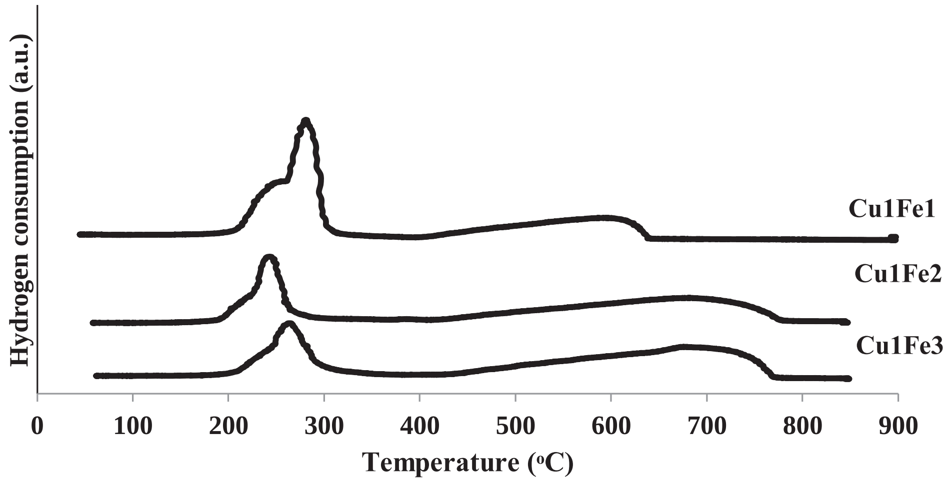

Figure 5.18 TPR profile of effect of ratio of copper and ferrite in precursor.

Catalytic evaluated performance for the methanol steam reforming

The catalysts evaluated performance of copper and ferrite ratio in precursor was prepared by flame spray pyrolysis step for the methanol steam reforming are shown in figure 5.19. Catalysts activity and hydrogen production rate increased with increasing copper content except the Cu1Fe1 catalyst because further increases copper loading resulted in formation of bulk CuO decreased catalysts activity. This is in line with TPR results (Fig. 5.18); a low-temperature peak appeared in the TPR profiles, attributed to the reduction of surface copper oxide species. At the highest copper loading, these CuO species are readily visible in the XRD pattern (Fig 5.14) [32] indicated that spinel structure is significant for methanol steam reforming. Which was reflected significance of copper spinel is better copper oxide because in methanol steam reforming, the spinel derived catalyst showed higher activity than then on spinel due to the higher dispersion of the Cu metal when was reduced [16]. Although spinel structure has important for this reaction but active site is also important so it season that 5Cu1Fe3-0.3M has the lower activity than 5Cu1Fe2-0.3M. In the other hand, the term of alternative energy sources was investigated, the 5Cu1Fe3-0.3M not should for methanol steam reforming because the highest CO selectivity. Suggest that, the effect of spinel structure have significant for methanol steam reforming as the Cu1Fe2 have higher activity than Cu1Fe1 even The Cu1Fe1 have the highest copper loading.

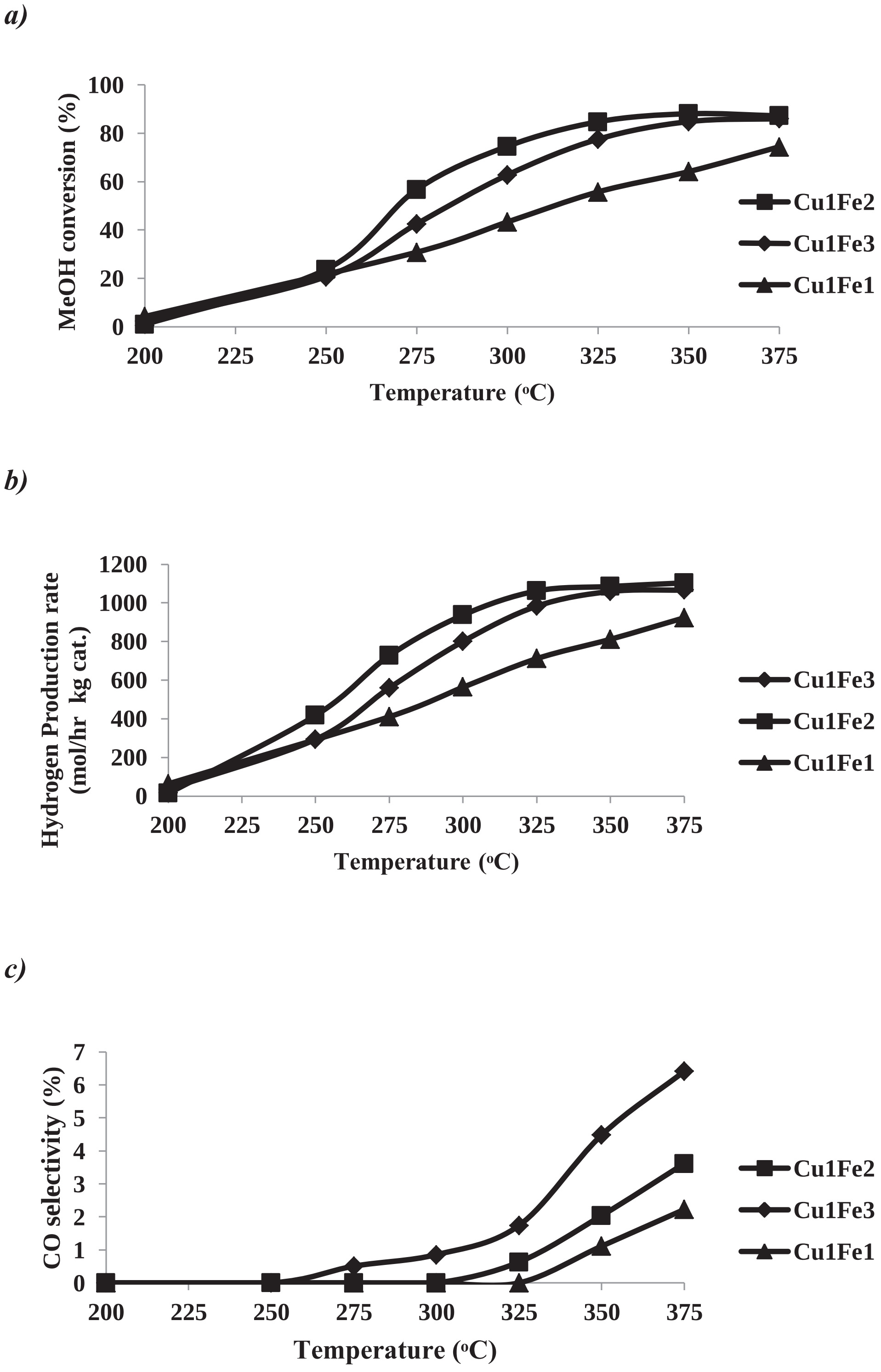

Figure 5.19 Effect of Cu:Fe ratio on a) MeOH conversion b) hydrogen production rate and c) CO selectivity over copper spinel in methanol steam reforming.

5.2.2 The effect of manganese loading.

The Physical and Chemical Properties of copper based spinel catalysts

- **The Phase Analysis by X-ray Diffraction**

The samples are denoted as CuXFeYMnZ when X: Y: Z = [Cu]:[Fe]:[Mn] and Y+Z = 2 because the Cu1Fe2 catalyst as the optimal the effect of copper and ferrite ratio from studied prior. The figure 5.20 shows XRD pattern of Cu-Fe-Mn catalysts structures. The peak of binary Cu-Mn system showed the $Cu_{1.5}Mn_{1.5}O_4$ as evidenced by the peak at ~36 and Mn_3O_4 phase. Indicated that the Cu-Mn system favored non-stoichiometric $Cu_xMn_{(3-x)}O_4$ when (X=1.2-1.5) phase in the equilibrium state[15]. Additional the peak of binary Cu-Fe catalyst show $CuFe_2O_4$ and CuO phase. Therefor investigation the ternary Cu-Fe-Mn system from the figure 5.20 show that the phase of $Cu_{1.5}Mn_{1.5}O_4$ appeared when high manganese loading as the Cu2Fe1Mn3 catalysts and decreased crystaliznity while increasing ferrite loading appeared $CuFe_2O_4$ phase as the Cu2Fe3Mn1 and Cu1Fe1Mn1 catalysts.

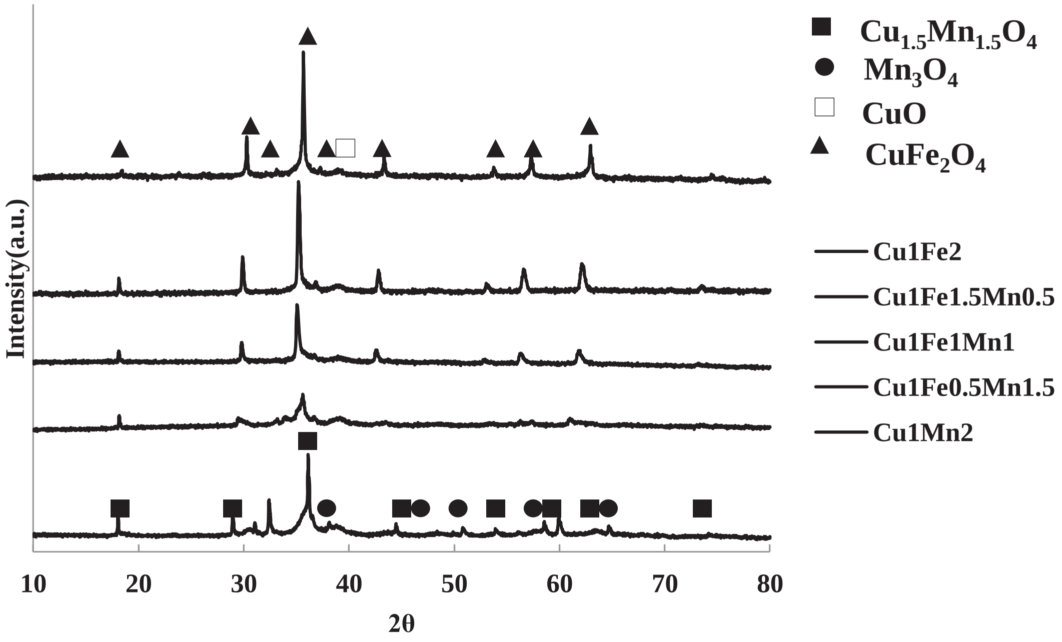

Figure 5.20 XRD pattern of effect of manganese loading in flame spary pylolysis preparation step.

- **The BET Surface Area and Pore Characteristics**

The specific surface area of Cu-Fe-Mn catalysts was shown in table 5.4. The result showed that the specific surface area of Cu2Fe1Mn3 was similar with Cu1Mn2 because they have comparable phase which confirmed from XRD pattern. However increasing copper content decreased specific surface area from 70 to 63.

Table 5.4 The BET surface area of effect of copper and ferrite ratio

Catalysts	**BET surface area (m^2/g)**
Cu1Fe2	**63**
Cu1Fe1.5Mn0.5	**69**
Cu1Fe1Mn1	**70**
Cu1Fe0.5Mn1.5	**49**
Cu1Mn2	**51**

- **The temperature programmed reduction**

The reducibility of Cu-Fe-Mn catalysts was investigated via TPR profile. All of catalysts are shown in figure 5.21. Main (310℃) and shoulder (290℃) peaks were observed for Cu1Mn2, ascribable to reduction of Cu^{2+} or Cu^{+} to Cu^{0}[15]. Additional from previous copper spinel in dimethyl ether steam reforming studied, the copper ferrite spinel show two main reduction peaks, Fe_2O_3 to Fe_3O_4 around 200-300°C and Fe_3O_4 to Fe^0 around 260°C and 450°C, respectively[11] and one shoulder peak was $CuFe_2O_4$ to Cu^0 and Fe_2O_3 around 200°C. Increasing manganese loading with peaks shifted higher temperature. From literature review of reducibility of Mn_2O_4 can reasonable. Generally, a two-step reduction profile of pure Mn_2O_4 has been reported. Before formation of the MnO phase, Mn_2O_3 is reduced to Mn_3O_4 at lower temperatures. Further reduction of MnO to metallic manganese does not occur up to 1000 for thermodynamic reasons[32] which higher $CuFe_2O_4$. As the peak area decreased, indicated that particle size and amount of reducible copper oxide decreased with the increased ferrite loading[15]. Tanaka et al[15] reported on the TPR profile of a Cu–Mn spinel oxide catalyst (Cu/Mn = 1/2, calcined at 900 °C)[15] which is similar in peak of $CuMn_2O_4$ in this work but from XRD pattern of $CuMn_2O_4$ (figure 5.20) show peak of CuO so TPR profile appear peak at temperature range of 250–300 °C of $CuMn_2O_4$ catalyst was ascribed to the reduction of CuO to metallic copper because the particles in flame spray pyrolysis were produced as a result of the competition between copper and manganese in gas phase which reacted with oxygen so appearance of copper manganese spinel, copper oxide and manganese spinel oxide maybe occur. This is based on the following evidence from XRD pattern (figure 5.20).

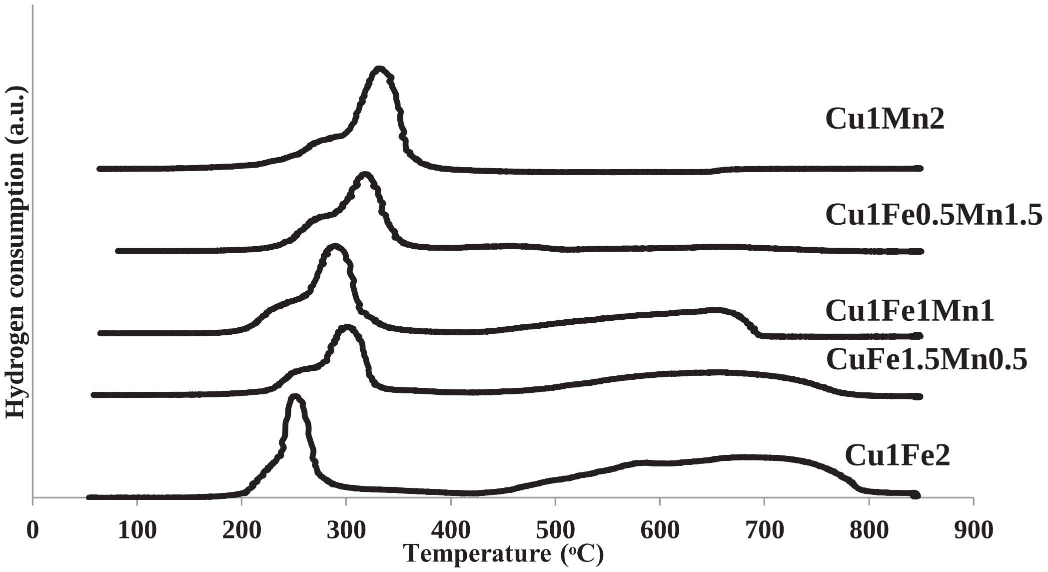

Figure 5.21 TPR profile of effect of ratio of copper and ferrite in precursor.

Catalytic evaluated performance for the methanol steam reforming

- **Methanol steam reforming via Cu1Fe2 and Cu1Mn2**

Figures 5.22a and 5.22b show methanol conversion and hydrogen production rate of Cu1Fe2 and Cu1Mn2 tested in methanol steam reforming. The results showed that the Cu1Fe2 has the highest methanol conversion but the Cu1Mn2 has the higher hydrogen production rate than Cu1Fe2. However the CO selectivity of Cu1Mn2 was higher than Cu1Fe2. This result can suggest that CO selectivity of Cu1Mn2 increased over the spinels contenting Mn presumably due to MeOH decomposition.

- **The effect of ferrite and manganese ratio**

From figure 5.23 show MeOH conversion, hydrogen production rate and CO selectivity of copper spinel in each condition. Mn loading showed higher catalytic activity and hydrogen production rate in methanol steam reforming suggest that the ternary Cu–Mn–Fe oxides improved MeOH conversion because showed higher catalytic activity for water gas shift reaction than the binary Cu1Mn2 catalyst [15]. However the binary Cu1Mn2 catalyst show the highest CO selectivity. The Cu1Fe1Mn1 show the highest MeOH conversion and hydrogen production rate because the Mn/Fe ratio affected the reducibility of copper and catalytic activity for WGSR.

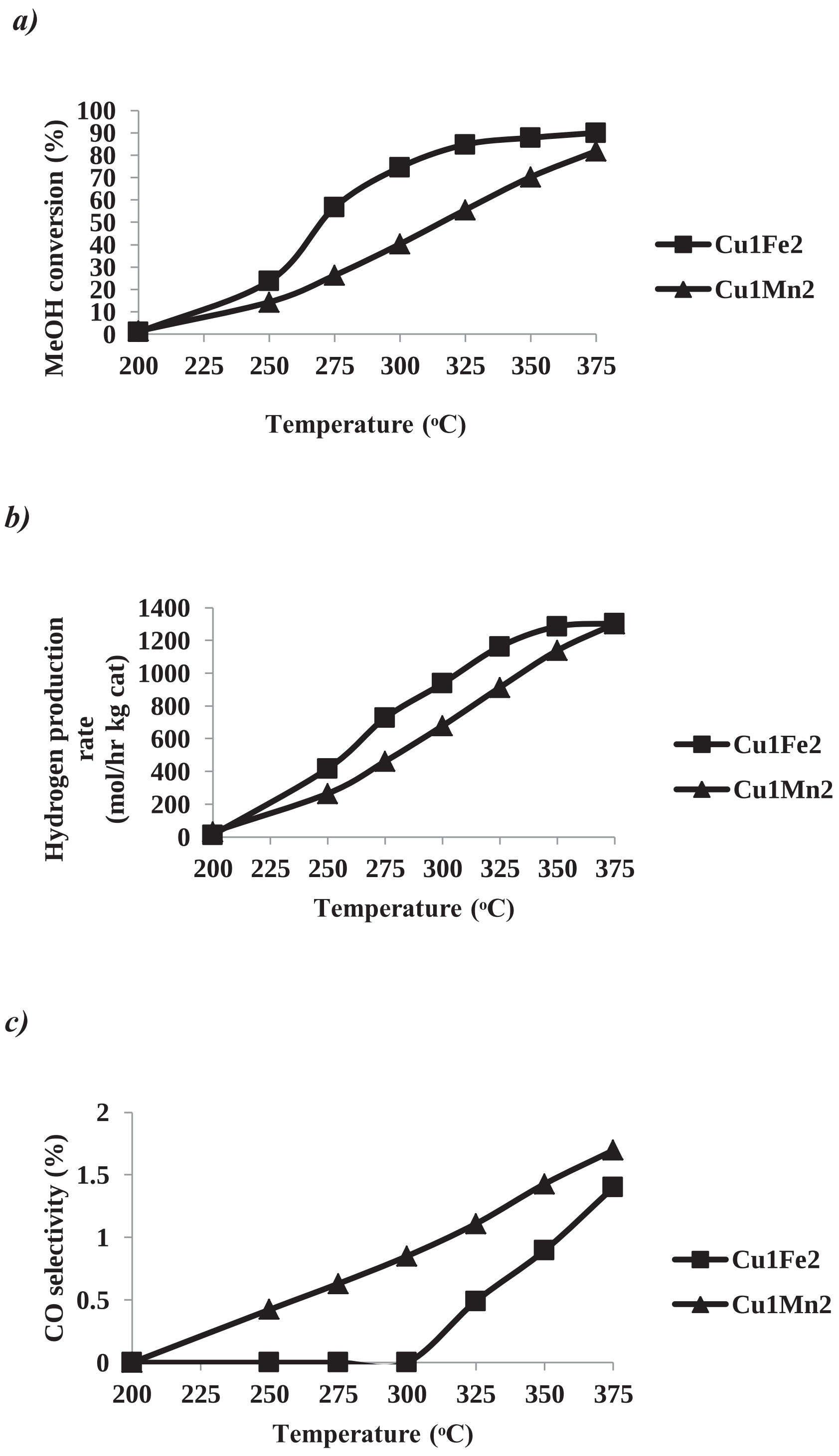

Figure 5.22 Effect of B site component (Fe,Mn) on a) MeOH conversion b) Hydrogen production rate and c) CO selectivity over spinel catalysts on methanol steam reforming.

a)

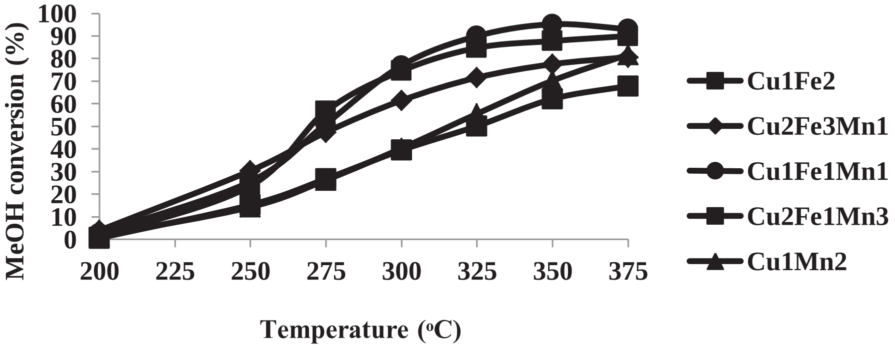

b)

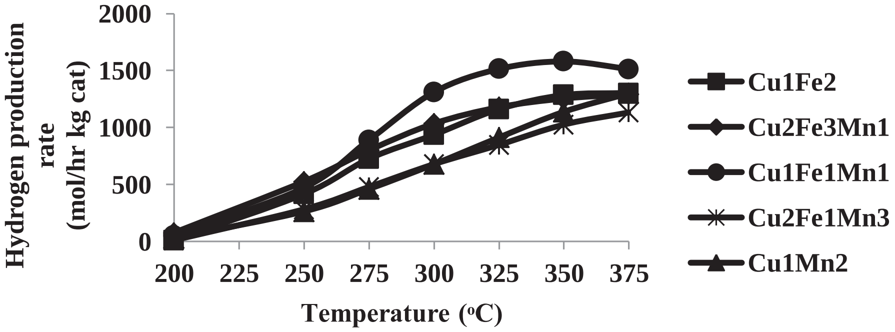

c)

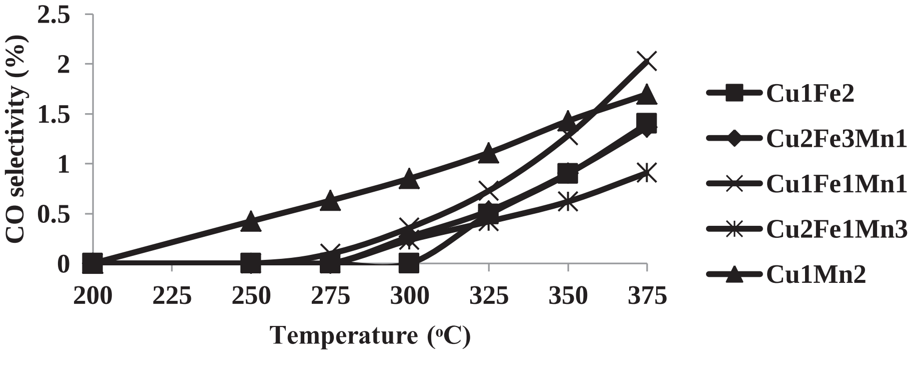

Figure 5.23 Effect of ratio of B site component (Fe:Mn) on a) MeOH conversion b) Hydrogen production rate and c) CO selectivity of Copper spinel of each condition over spinel catalysts on methanol steam reforming.

5.3 The effect of temperature reduction

Effect of reduction pretreatment on the catalytic activity of the composite catalysts of $CuFe_2O_4$ in each condition for methanol steam reforming was tested under the reaction conditions of S/C = 2.0. Prior to methanol steam reforming reaction, the composites were reduced in 10% H_2/N_2 for 1 h at 200, 300 and 350°C. This section was divided two part consist of the effect of temperature reduction and the effect of time in reduction.

The Physical and Chemical Properties of copper based spinel catalysts

- **The Phase Analysis by X-ray Diffraction**

Figure 5.24 shows XRD pattern of catalysts after reduction at each temperature. The fresh catalyst before reduction shows a highly crystallized copper ferrite spinel phase, after reduced at 200, 300 and 350, copper ferrite composed of two phases of metallic Cu and Fe_3O_4. The main peaks for Cu at 2θ = 43.38° and 50.48°. The Cu crystallite size calculated using Scherrer formula at the 2θ = 43.38°. The effect of temperature reduction affects that intensity of Fe_3O_4 and copper metal change. Increasing the temperature reduction increased crystallite size of metallic Cu and Fe_3O_4 as the crystallite size increased in keeping with the reduction temperature: 24, 27, 51, and 60 nm for the catalysts reduced at 250, 350, 450, and 600 °C, respectively[11]. Addition, effect of reduction time also affected to Fe_3O_4 and copper metal. After reduced copper ferrite at 200°C for 3h, intensity of peak Fe_3O_4 and copper metal also increased.

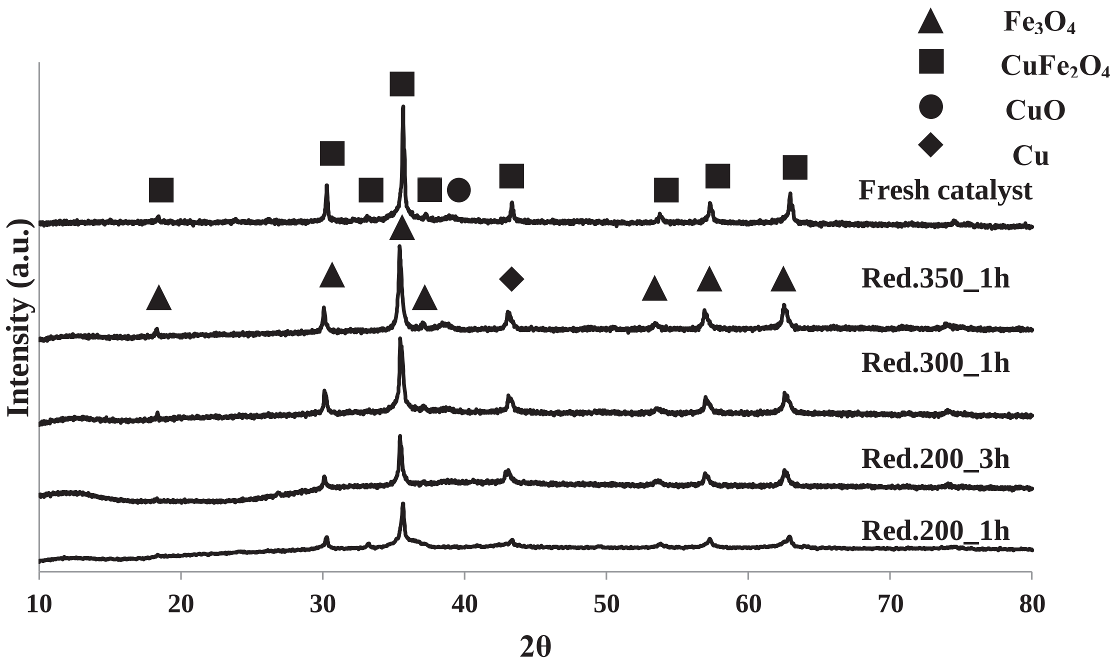

Figure 5.24 XRD pattern of catalysts after reduction at each temperature.

- **The temperature programmed reduction**

From figure 5.26 show hydrogen TPR profiles of $CuFe_2O_4$ at each temperature reduction. Normally, the $CuFe_2O_4$ sample exhibited two distinct peaks showing maximum at 250 °C and 580 °C. The peaks appearing in the temperature range of 200–350 °C were ascribed to the reduction of $CuFe_2O_4$ to metallic Cu and Fe_2O_3, and to the subsequent reduction of Fe_2O_3 to Fe_3O_4. It is hard to define a clear boundary between each of the reduction steps. The iron oxides continued to be reduced to metallic Fe via FeO, according to the peak appearing at higher temperature [11]. Therefore, when increased temperature reduction the TPR peaks appearing in the temperature range of 200–350 °C will decrease because the reduction of $CuFe_2O_4$ to metallic Cu and Fe_2O_3 prior. However, TPR peaks appearing in the temperature range of 450–780 °C will constant because at temperature 200, 300 and 350, the iron oxides cannot reduce to metallic Fe via FeO.

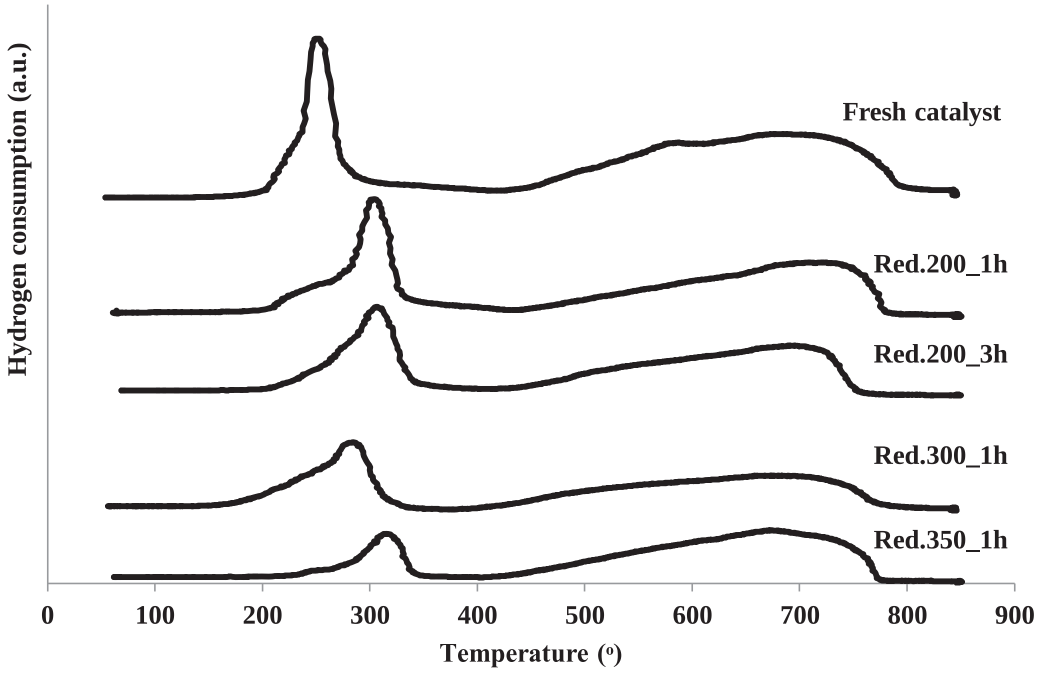

Figure 5.25 TPR profile of catalysts after reduction each temperature.

Catalytic evaluated performance for the methanol steam reforming

Figure 5.27 shows MeOH conversion of reduced and unreduced catalysts at temperature reduction 200-350 °C. Result show that, MeOH conversion over the catalysts was increased considerably by increasing the reduction temperature to unreduced and 300 °C and slight drop in the activity was observed over the catalyst reduced at 350 °C. However, no found that degradation of the catalytic activity proceeded because from literate review of K.Faungnawakij et al. (2008) found that degradation of the catalytic activity proceeded significantly over both catalysts during dimethyl ether steam reforming for 25 h, and more severely over the sample reduced at 600 °C [11]. From figure 5.24 shows XRD pattern of catalysts after reaction at each temperature which can evident for no degradation of the catalytic activity because the phase of Fe_3O_4 and Cu metal do not change over all catalysts but also increase crystallinity of catalysts.

a)

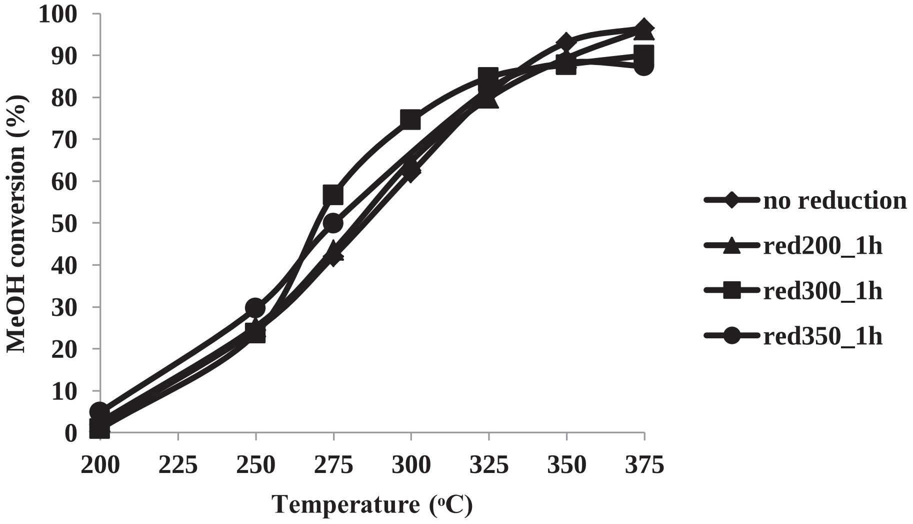

b)

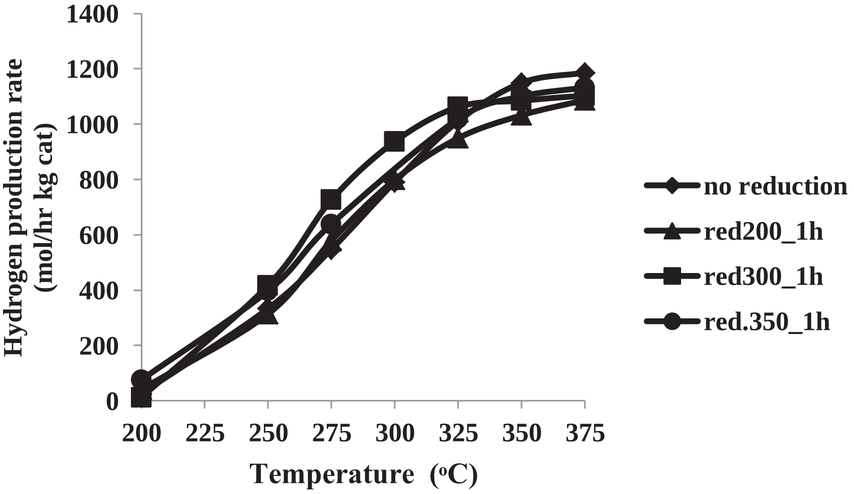

Figure 5.26 Effect of temperature reduction on a) MeOH conversion and b) hydrogen production rate of Copper spinel and c) CO selectivity over spinel catalysts on methanol steam reforming.

a)

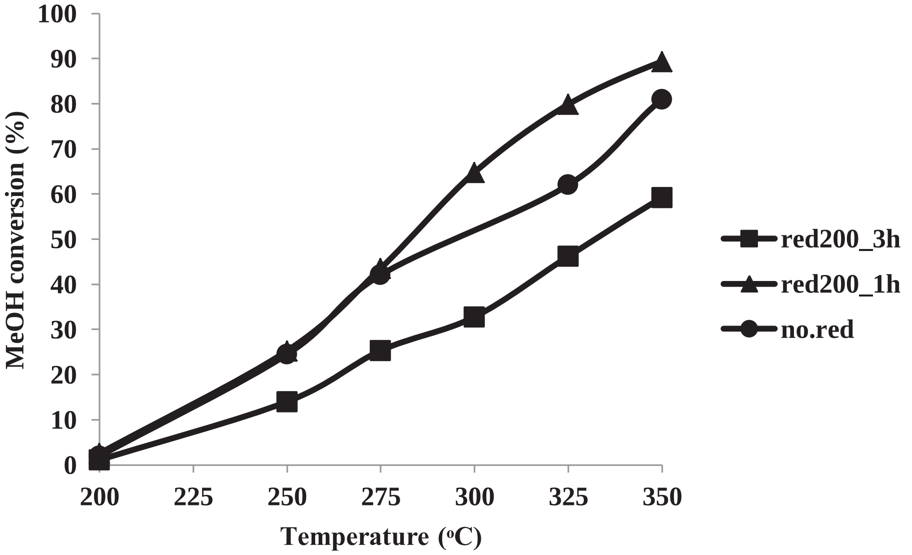

b)

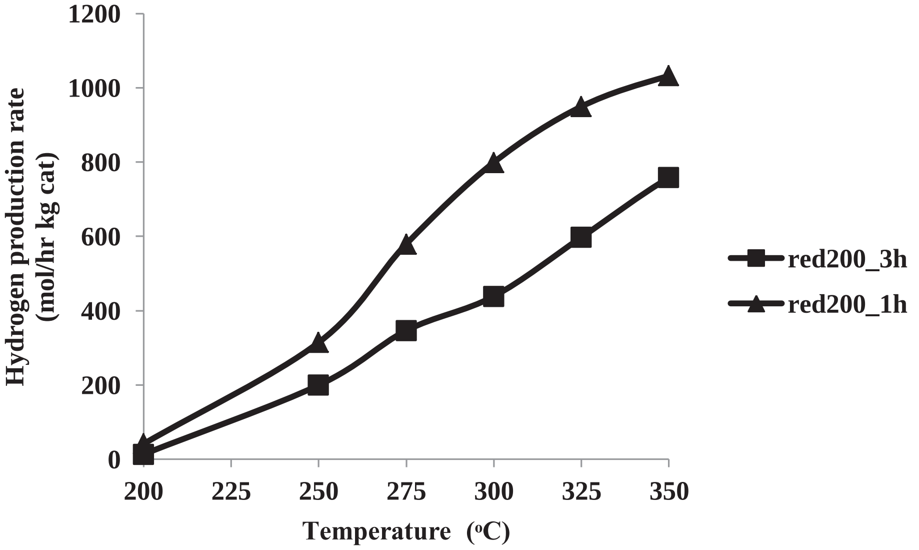

Figure 5.27 Effect of time of temperature reduction a) MeOH conversion and b) hydrogen production over spinel catalysts on methanol steam reforming..

5.4 The catalysts evaluation in dimethyl ether steam reforming

The catalysts evaluation were tested by dimethyl ether steam reforming, study the catalytic performance of the flame-made catalysts such as activity and selectivity of hydrogen on dimethyl ether steam reforming reaction by varied reaction‘s temperature from 200-375℃. The effect copper and ferrite ratio has been investigated. Figure 5.29 showed catalytic behaviors over spinel catalysts mixed with $\gamma-Al_2O_3$. The results showed that the catalytic performance of the flame-made catalysts (Cu1Fe2+ALO8) and the catalysts synthesized from critic acid method (Cu1Fe2(900)) [6] were different. Normally side reduction of dimethyl ether steam reforming consists of dimethyl ether decomposition and r-WGSR; both of reaction produced CO and CH_4 while r-WGSR will decrease hydrogen production rate. The Cu1Fe2+ALO8 gave the highest hydrogen production and the highest CH_4 selectivity at high temperature. The Cu1Fe3+ALO8 showed lowest activity. The higher activity of the Cu1Fe2(900) might be from the effect of high temperature calcination. The flame-made catalysts might require proper calcination condition to improve its performance.

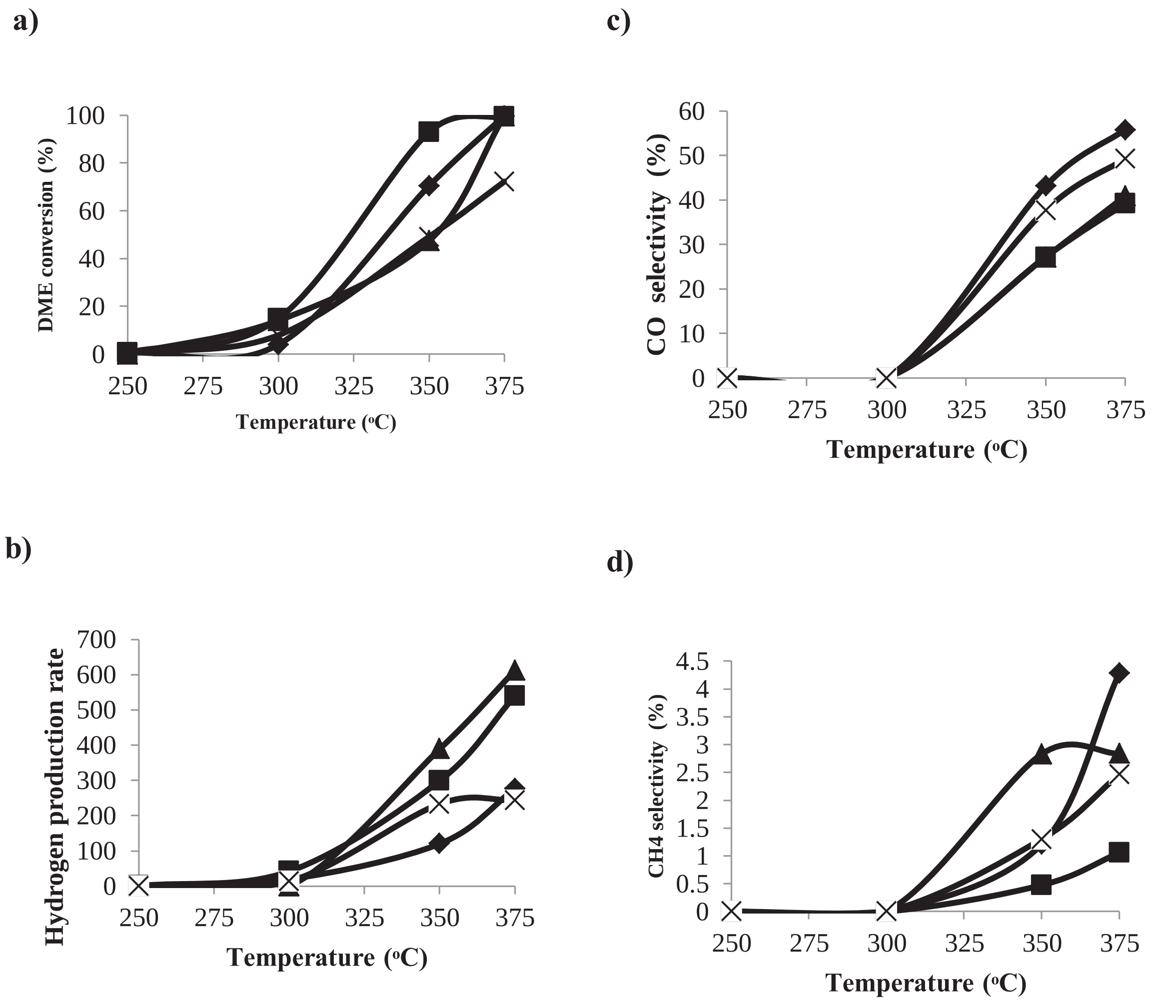

Figure 5.28 Effect of Cu:Fe ratio on a) MeOH conversion b) hydrogen production rate of Copper spinel and c) CO selectivity over spinel catalysts on dimethyl ether steam reforming; Cu1Fe1+ALO8, ♦, Cu1Fe2(900)+ALO8, ■, Cu1Fe2_ALO8 Cu1Fe2+ALO8, ▲ and Cu1Fe3+ALO8, ×.

CHAPTER 6

CONCLUSIONS AND RECOMMENDATION

In this research, the catalytic performance of copper based spinel nanocatalysts using flame spray pyrolysis (FSP) technique, optinal condition such as effect of precursor concentration and effect of precursor feed rate, the effect of copper and errite ratio on the Methanal steam reforming were investigated. The experimental conclusions were summarized as follows:

1. Flame spray pyrolysis can synthesize the copper ferrite spinnel based catalysts in the cubic phase.
2. The effect of precursor types shows that crystallize size of Cu1Fe2_NO much more than Cu1Fe2_MIX two times.
3. The Cu1Fe2_NO shows the superior methanol conversion and hydrogen production rate than the Cu1Fe2_MIX because the Cu1Fe2_NO completely reduced faster than Cu1Fe2_MIX.
4. Increasing the precursor concentration and precursor feed rate continuously increases the product particle diameter as the particle concentration and residence time at high temperatures increase.
5. The 5Cu1Fe2-0.5M provided superior catalytic activity hydrogen production rate and CO selectivity in methanol reforming. Even 5Cu1Fe2-0.3M not provided superior catalytic activity and hydrogen production rate but it shows the smallest CO selectivity. So it is the optimal catalysts in this research.
6. Increasing copper loading increased particle size because effect of CuO occur while The Cu1Fe1 have the largest particle size.
7. The 5-Cu1Fe2-0.3M showed the highest activity while 5-Cu1Fe1-0.3M has lower than one because it catalysts has CuO more than 5-Cu1Fe2-0.3M catalyst indicated that spinel structure is significant for methanol steam reforming.

8. The effect Mn/Fe ratio in the Cu–Mn–Fe catalysts influenced reducibility of copper oxide after reduction of spinel phases. Increasing Mn loading reduction behavior increased.
9. The phase of $Cu_{1.5}Mn_{1.5}O_4$ appeared when high manganese loading as the Cu2Fe1Mn3 catalysts and decreased crystaliznity.
10. Mn loading into $CuFe_2O_4$ improve methanol conversion and hydrogen production rate.
11. Optimized Cu1Mn1Fe1 is the best catalytic activity. Not only particle size and amount of Cu but also active supports are significant to improve r-WGSR activity.

Bibliography

1. Strobel, R., A. Alfons, and S.E. Pratsinis, *Aerosol flame synthesis of catalysts.* Advanced Powder Technology, 2006. **17**(5): p. 457-480.
2. Piacentini, M.S., R. Maciejewski, M. Pratsinis, S. E. Baiker, A., *Flame-made Pt-Ba/*Al_2O_3 *catalysts: Structural properties and behavior in lean-*NO_x *storage-reduction.* Journal of Catalysis, 2006. **243**(1): p. 43-56.
3. Symalla, M.O., Drochner, A., Vogel, H., Bachel, R., Pratsinis, S. E., Baiker, A., *Structure and NOx storage behaviour of flame-made* $BaCO_3$ *and Pt/*$BaCO_3$ *nanoparticles.* Applied Catalysis B: Environmental, 2009. **89**(1-2): p. 41-48.
4. Height, M.J.P., Sotiris E. Mekasuwandumrong, Okorn Praserthdam, Piyasan, *Ag-ZnO catalysts for UV-photodegradation of methylene blue.* Applied Catalysis B: Environmental, 2006. **63**(3-4): p. 305-312.
5. S. Pisduangdaw, J.P., C. Methastidsook, C. Chaisuk, K. Faungnawakij, P. Praserthdam, O. Mekasuwandumrong, *Characteristics and catalytic properties of Pt-Sn/*Al_2O_3 *nanoparticles synthesized by one-step flame spray pyrolysis in the dehydrogenation of propane.* Applied Catalysis A, 2009.
6. Faungnawakij, K., R. Kikuchi, and K. Eguchi, *Thermodynamic analysis of carbon formation boundary and reforming performance for steam reforming of dimethyl ether.* Journal of Power Sources, 2007. **164**(1): p. 73-79.
7. Faungnawakij, K., R. Kikuchi, and K. Eguchi, *Thermodynamic evaluation of methanol steam reforming for hydrogen production.* Journal of Power Sources, 2006. **161**(1): p. 87-94.
8. Faungnawakij, K., Kikuchi, R., Matsui, T., Fukunaga, T., Eguchi, K, *A comparative study of solid acids in hydrolysis and steam reforming of dimethyl ether.* Applied Catalysis A: General, 2007. **333**(1): p. 114-121.
9. Shimoda, N., Faungnawakij, K., Kikuchi, R., Fukunaga, T., Eguchi, K., *Catalytic performance enhancement by heat treatment of* $CuFe_2O_4$ *spinel and [gamma]-alumina composite catalysts for steam reforming of dimethyl ether.* Applied Catalysis A: General, 2009. **365**(1): p. 71-78.
10. Faungnawakij, K., Kikuchi, Ryuji, Fukunaga, Tetsuya, Eguchi, Koichi, *Catalytic hydrogen production from dimethyl ether over* $CuFe_2O_4$ *spinel-based composites: Hydrogen reduction and metal dopant effects.* Catalysis Today, 2008. **138**(3-4): p. 157-161.
11. Faungnawakij, K., Tanaka, Y., Shimoda, N., Fukunaga, T., Kikuchi., Eguchi, K., *Hydrogen production from dimethyl ether steam reforming over composite catalysts of copper ferrite spinel and alumina.* Applied Catalysis B: Environmental, 2007. **74**(1-2): p. 144-151.
12. Faungnawakij, K., Fukunaga, T., Kikuchi, R., Eguchi, K., *Deactivation and regeneration behaviors of copper spinel-alumina composite catalysts in steam reforming of dimethyl ether.* Journal of Catalysis, 2008. **256**(1): p. 37-44.

Bibliography

13. Faungnawakij, K., Shimoda, N., Fukunaga, T., Kikuchi, R., Eguchi, K., *Cu-based spinel catalysts CuB_2O_4 (B = Fe, Mn, Cr, Ga, Al, $Fe_{0.75}Mn_{0.25}$) for steam reforming of dimethyl ether.* Applied Catalysis A: General, 2008. **341**(1-2): p. 139-145.
14. Y. Tanaka, T.T., R. Kikuchi, K. Eguchi,, *Influence of preparation method and additive for Cu-Mn spinel oxide catalyst on water gas shift reaction of reformed fuels.* Applied Catalysis A: General, 2005. **279**(1-2): p. 59-66.
15. Fukunaga, T., Ryumon, N., Ichikuni, N., Shimazu, S., *Characterization of CuMn-spinel catalyst for methanol steam reforming.* Catalysis Communications, 2009. **10**(14): p. 1800-1803.
16. Houteit, A., et al., *Production of hydrogen by steam reforming of methanol over copper-based catalysts: The effect of cesium doping.* Applied Catalysis A: General, 2006. **306**: p. 22-28.
17. Roger Mueller, L.M.-a., Sotiris E. Pratsini*, *Nanoparticle synthesis at high production rates by fame spray pyrolysis.* Chemical Engineering Science, 2003. **58**: p. 1969-1976.
18. Jang, H.D., et al., *Synthesis of SiO_2 nanoparticles from sprayed droplets of tetraethylorthosilicate by the flame spray pyrolysis.* Current Applied Physics, 2006. **6, Supplement 1**(0): p. e110-e113.
19. N.v. Vegten, T.B., F. Krumeich, W. Kleist, B. Alfons, *Flame-made $MgAl_{2-x}M_xO_4$ (M=Mn, Fe, Co) mixed oxides: structural properties and catalytic behavior in methane combustion.* Applied Catalysis B: Environmental, 2010. **97**(3-4): p. 398-406.
20. I. S. AHMED FARAG, M.A.A., S. M. HAMMAD, A. M. MOUSTAFA, *Application of Rietveld Method to the Structural Characteristics of Substituted Copper Ferrite Compounds.* Cryst. Res. Technol., 2001. **36**: p. 85-92.
21. G.F.Goya, H.R.Rechenberg, J.Z.J., *Structural and magnetic properties of ball milled copper ferrite.* J.Appl.Phys., 1998. **84**: p. 1101-1108.
22. R.Jossen, *Controlled synthesis of mixed oxide particles in flame spray pyrolysis.* Dissertation 16401, ETH, Zurich 2006.
23. G.Saracco, F.G., D.Mazza and G.Baldi, *New method for catalyst powder manufacturing based on solvent combustion.* J.Therm.Anal, 1999. **Calorim. 56**: p. 1435–1442.
24. R. Strobel, F.K., W.J Stark, S.E. Pratsinis, A. Baiker, *Flame spray synthesis of Pd/Al_2O_3 catalysts and their behavior in enantioselective hydrogenation.* Journal of Catalysis, 2004. **222**(2): p. 307-314.
25. Mudler, L., et al., *Controlled synthesis of nanostructured particles by flame spray pyrolysis.* Journal of Aerosol Science, 2002. **33**(2): p. 369-389.
26. Roger Mueller, L.M.-a., Sotiris E. Pratsinis*, *Nanoparticle synthesis at high production rates by fame spray pyrolysis.* Chemical Engineering Science, 2003. **58**: p. 1969-1976.

Bibliography

27. Okorn Mekasuwandumronga, S.P., Bunjerd Jongsomjit, Artiwan Shotiprukb, Joongjai Panpranotb,*, *Influence of flame conditions on the dispersion of Pd on the flame spray-derived Pd/TiO_2 nanoparticles.* Powder Technology, 2011. **210**: p. 328-331.
28. Papavasiliou, J., G.A. , T.I. , *Combined steam reforming of methanol over Cu–Mn spinel oxide catalysts.* Journal of Catalysis, 2007. **251**: p. 7-20.
29. G.F. Goyaand, H.R.R., J.Z.Jiang, *Structural and magnetic properties of ball milled copper ferrite.* J.Appl.Phys., 1998. **84**: p. 1101-1108.
30. G.J. Hutchings, A.A.M., R.W. Joyner, M.R.H. Siddiqui, S.H. Taylor, *Effect of preparation conditions on the catalytic performance of copper manganese oxide catalysts for CO oxidation.* Applied Catalysis A: General, 1998. **166**(1): p. 143-152.
31. Lin, H.-Y., Y.-W. Chen, C. Li, *The mechanism of reduction of iron oxide by hydrogen.* Thermochimica Acta, 2003. **400**(1-2): p. 61-67.
32. Y.Tanaka, [a,]T.U., [a] R. Kikuchi,[a] T. Takeguchi,[a] K. Sasaki,[b] and K. Eguchi [a,]*, *Water gas shift reaction for the reformed fuels over Cu/MnO catalysts prepared via spinel-type oxide.* Journal of Catalysis, 2003. **215**: p. 271-278.
33. H. Purnama [a,] T.R.[a.,] *, R.E. Jentoft [a], H. Soerijanto [a], R. Schlögl [a], R. Schomäcker [b], *CO formation/selectivity for steam reforming of methanol with a commercial CuO/ZnO/Al_2O_3 catalyst.* Applied Catalysis A: General, 2004. **259**: p. 83-94.
34. Yohei Tanaka, R.K., Tatsuya Takeguchi, Koichi Eguchi, *Steam reforming of dimethyl ether over composite catalysts of g-Al_2O_3 and Cu-based spinel.* Applied Catalysis B, 2005. **57**(Environmental): p. 211-222.
35. DanielR. Palo*, R.A.D.a.J.D.H., *Methanol Steam Reforming for Hydrogen Production.* Chem.Rev., 2007. **107**(10): p. 3992−4021.
36. Eguchi, K.S., N. Faungnawakij, K. Matsui, T. Kikuchi, R. Kawashima, S., *Transmission electron microscopic observation on reduction process of copper-iron spinel catalyst for steam reforming of dimethyl ether.* Applied Catalysis B: Environmental, 2008. **80**(1-2): p. 156-167.
37. Jingsheng Jia [a, b.,] Jin Zhou [a], Chunxi Zhang [a], Zhongshan Yuan [a], Shujuan Wang [a], Lei Cao [a,b], Shudong Wang [a,]*, *Preparation and characterization of Ir-based catalysts on metallic supports for high-temperature steam reforming of methanol.* Applied Catalysis A, 2008. **341**: p. 1-7.
38. Khan, A. and P.G. Smirniotis, *Relationship between temperature-programmed reduction profile and activity of modified ferrite-based catalysts for WGS reaction.* Journal of Molecular Catalysis A: Chemical, 2008. **280**(1-2): p. 43-51.
39. Samuel D. Jones, L.M.N., Helena E. Hagelin-Weaver*, *Steam reforming of methanol using Cu-ZnO catalysts supported on nanoparticle alumina.* Applied Catalysis B, 2008. **84**: p. 631-642.
40. Kajornsak Faungnawakij, N.S., Tetsuya Fukunaga, Ryuji Kikuchi ,KoichiEguchi, *Crystal structure and surface species of $CuFe_2O_4$ spinel catalysts in steam reforming of dimethyl ether.* Applied Catalysis B, 2009. **92**(Environmental): p. 341-350.

Bibliography

41. N.v. Vegten, T.B., F. Krumeich, W. Kleist, B. Alfons, *Flame-made $MgAl_{2-x}M_xO_4$ (M=Mn, Fe, Co) mixed oxides: structural properties and catalytic behavior in methane combustion.* Applied Catalysis B: Environmental, 2010. **97**(3-4): p. 398-406.
42. Zielinski, J.Z., I. Znak, L. Kaszkur, Zbigniew, *Reduction of Fe_2O_3 with hydrogen.* Applied Catalysis A: General, 2010. **381**(1-2): p. 191-196.
43. Chaisuk, C., Boonpitak, Pornpoj, Panpranot, Joongjai, Mekasuwandumrong, Okorn, *Effects of Co dopants and flame conditions on the formation of Co/ZrO_2 nanoparticles by flame spray pyrolysis and their catalytic properties in CO hydrogenation.* Catalysis Communications, 2011. **12**(10): p. 917-922.
44. Yohei Tanaka, [a.]T.U., [a] Ryuji Kikuchi,[a] Tatsuya Takeguchi,[a] Kazunari Sasaki,[b] and Koichi Eguchi [a,*], *Water gas shift reaction for the reformed fuels over Cu/MnO catalysts prepared via spinel-type oxide.* Journal of Catalysis, 2003. **215**: p. 271-278.

Appendix A

CALCULATION FOR CATALYST PREPARATION

APPENDIX A

CALCULATION FOR CATALYST PREPARATION

Table A.1 Chemical Properties of Cu spinel

Metal or Metal oxide	MW of metal (g/mol)	Metal Precursor	MW of Metal Precursor (g/mol)	Density (g/cm^3)	Metal content (%)
Cu	63.546	$Cu(NO_3)_2{\cdot}3H_2O$	241.5	2.32	99
Fe	55.845	$Fe(NO_3)_2{\cdot}9H_2O$	403.99	1.68	98
		$Fe(C_5H_7O_2)_3$		5.24	99
Mn	54.938	$Mn(NO_3)_2{\cdot}4H_2O$	178.95	1.54	99
Al_2O_3	101.96	$Al(OCH(CH_3)C_2H_5)_3$	246.33	0.96	97

A.1 Calculation of catalyst prepared by flame spray pyrolysis

0.3 M solution was used as precursor for catalyst preparation by flame spray pyrolysis is shown as follows:

Example: Calculation for the preparation of the 1:2$CuFe_2O_4$ catalysts, copper nitrate [Cu $(NO_3)_2{\cdot}3H_2O$] (Sigma-Aldrich) and iron nitrate [Fe $(NO_3)_2{\cdot}9H_2O$] (Sigma-Aldrich) were used as precursor and diluted with ethanol (J.T. baker) to a 0.3 M solution.

Basis 1000 ml precursor solution 0.3 M

Based on the composition of the catalyst will be as follows:

Total mole : mol $= \frac{\text{concentration (M)}\times\text{volume (ml)}}{1000}$

$\therefore$ Total mol $= \frac{(0.3M)\times(1000ml)}{1000} = 0.3$ mol

From 1:2$CuFe_2O_4$ has total metal = 3 parts

So, Cu metal has 1/3 $= \frac{1}{3}\times 0.3$ mol $= 0.1$ mol

Fe metal has 2/3 $= \frac{2}{3}\times 0.3\, mol$ $= 0.2$ mol

$\therefore$ Precursor Cu $= \frac{(0.1mol)\times(241.5\, {}^{g}/_{mol})}{0.99}$ =24.3939gCu

$\therefore$ Precursor Fe = $\frac{(0.2mol)\times(404\,{}^{g}/_{mol})}{0.98}$ = 82.4490gFe

A.2 Calculation of feed methanol mix with steam

From $\mathrm{MeOH} + \mathrm{H_2O} \rightarrow 3\mathrm{H_2} + \mathrm{CO_2}$

Basis Total flow of steam and MeOH are 100 ml/min and

By ratio of MeOH: H_2O = 1:2 by mol

Table A.2 Chemical Properties of feed

Substance	MW of metal (g/mol)	Formula.	Density (g/cm^3)
water	18	H_2O	1.0000
Methanol (MeOH)	32	CH_3OH	0.7718

- Find the moles of steam and MeOH in gas phase.

Basis: 1 min, Gas 1 mol have a volume = 24450 ml (ideal gas)

In gas phase: volume of gas 24450 ml has a 1 mol of gas

volume of gas 100 ml has $\frac{(100ml)\times(1mol)}{24450ml}$ mol

= 0.004089 mol

= 0.0041 mol

From MeOH: H_2O = 1:2 by mol = 3 parts

$\therefore$ In gas phase has MeOH $= \frac{1}{3}(0.0041\text{ mol}) = 0.0014\text{ mol}$

$\therefore$ In gas phase has steam $= \frac{2}{3}(0.0041\text{ mol}) = 0.0027\text{ mol}$

- Determine the amount of water and MeOH has been fed into HPLC pump.

General $\mathrm{Mol_{gas}}=\mathrm{Mol_{liquid}}$

So, in liguid phase: H_2O = $\frac{(0.0027\text{mol})\times(18\text{g/mol})}{(1\text{g/cm}^3)}$ = 0.0486 cm^3

MeOH = $\frac{(0.0014\text{mol})\times(32\text{g/mol})}{(0.7718\text{g/cm}^3)}$ = 0.0580 cm^3

∴ Total flow in liquid phase; 0.0486 + 0.0580 = 0.1066 ml (fed into HPLC pump)

- Determine flow of water and MeOH in liquid phase

MeOH = (0.0014 mol)(24450 ml/mol) = 34.23 ml/min≈ 34 ml/min

H_2O = (0.0027 mol)(24450 ml/mol) = 66.015 ml/min ≈ 66 ml/min

Total flow in gas phase; 34.23+66.015= 100.245 ml/min ≈ 100 ml/min

Appendix B

CALCULATION OF THE CRYSTALLITE SIZE

APPENDIX B

CALCULATION OF THE CRYSTALLITE SIZE

Calculation of the crystallite size by Debye-Scherrer equation

The crystallite size was calculated from the half-height width of the diffraction peak of XRD pattern using the Debye-Scherrer equation.

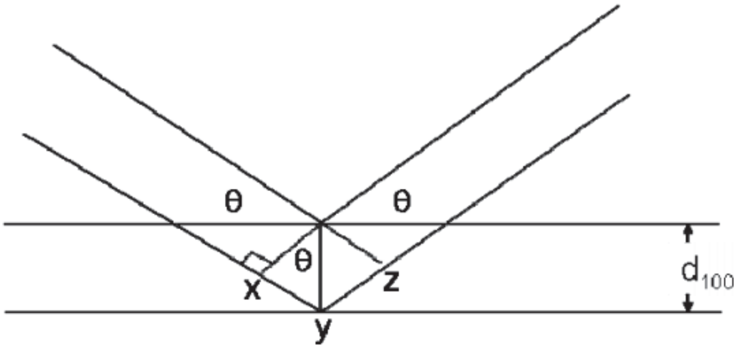

Figure B.1 Derivation of Bragg's Law for X-ray diffraction

$$xy = yz = d \sin\theta$$

Thus $\quad xyz = 2\ d \sin\theta \quad$ Bragg's Law

But $\quad xyz = n\lambda$

Therefore $\quad 2\ d \sin\theta = n\lambda$

$$d = \frac{n\lambda}{2 \sin\theta}$$

The Bragg's Law was derived to B.1

From Scherrer equation:

$$D = \frac{K\lambda}{\beta \cos \theta} \tag{B.1}$$

Where D = Crystallite size, Å

K = Crystallite-shape factor = 0.9

λ = X-ray wavelength, 1.5418 Å for CuKα

θ = Observed peak angle, degree

β = X-ray diffraction broadening, radian

The X-ray diffraction broadening (β) is the pure width of powder diffraction free from all broadening due to the experimental equipment. The α-alumina is used as a standard sample to observe the instrumental broadening since its crystallite size is larger than 2000 Å. The X-ray diffraction broadening (β) can be obtained by using Warren's formula.

From Warren's formula:

$$\beta = \sqrt{B_M^2 - B_S^2} \tag{B.2}$$

Where B_M= the measured peak width in radians at half peak height.

B_S= the corresponding width of the standard material.

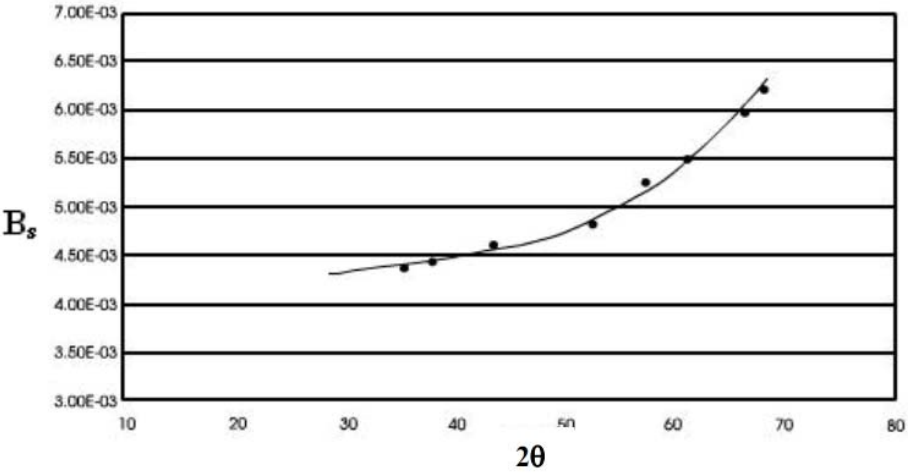

Figure B.2 The plot indicating the value of line broadening due to the equipment. The data were obtained by using α-alumina as a standard

APPENDIX C

Calibration curve for gaseous product

APPENDIX C

Calibration curve for gaseous product

C-1 Calibration curve for nitrogen

C.1 Average peak area of nitrogen (99.9% N_2)

Number	Peak Area
0	0
1	413759.2
2	414434.3
3	413676.4
4	413992
5	414416.1
6	413443.8
avg.	413953.6

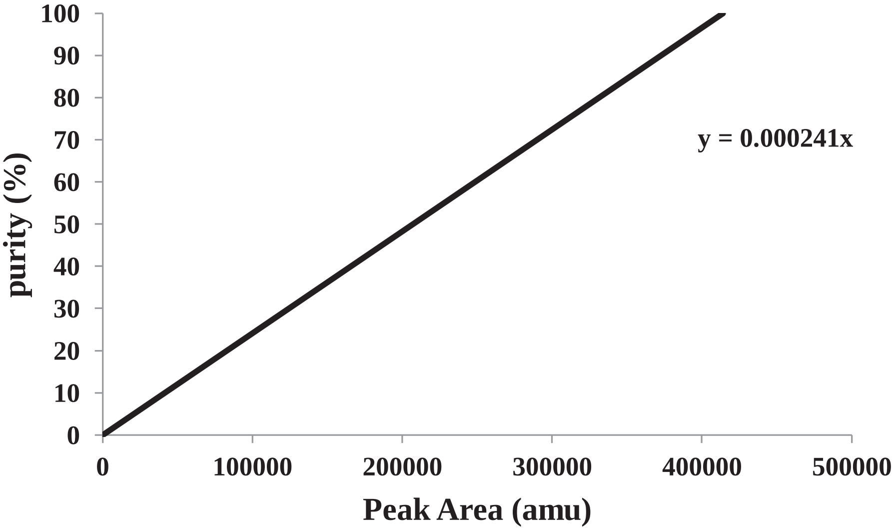

Figure C.1 Calibration curve for nitrogen 99.9%

C-2 Calibration curve for hydrogen

C.2 Average peak area of hydrogen 30%H_2/N_2(99.999% H_2)

Number	Peak Area
1	1146795
2	1235103
3	1259271
4	1273243
5	1281848
6	1284511
7	1286472
8	1285341
9	1285778
avg.	1284790

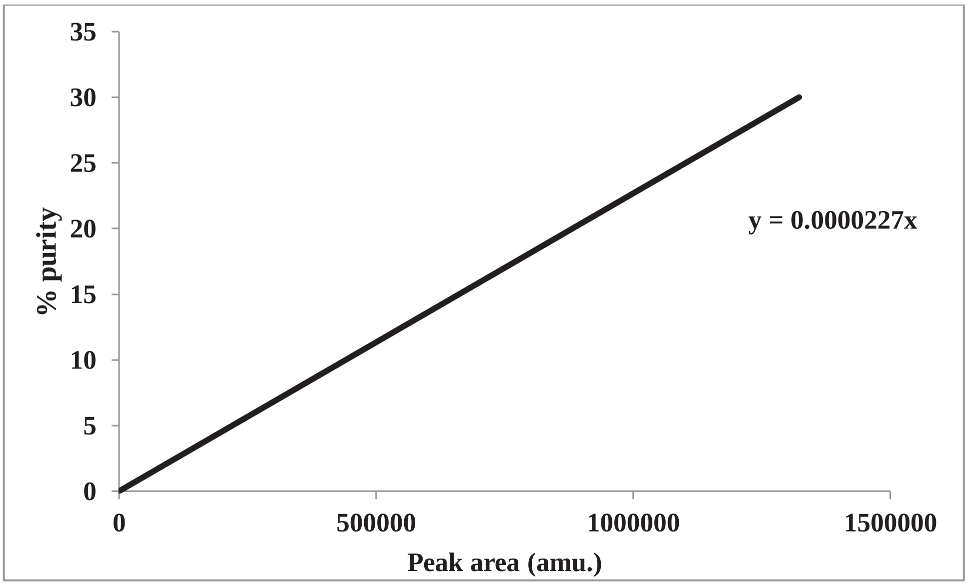

Figure C.2 Calibration curve for hydrogen 30%H_2/N_2(99.999% H_2)

C-3 Calibration curve for carbon monoxide

C.3 Average peak area of carbon monoxide 99.5%

Number	Peak Area
1	449739.0
2	446961.4
3	444807.0
4	440942.0
5	438159.8
avg.	444121.84

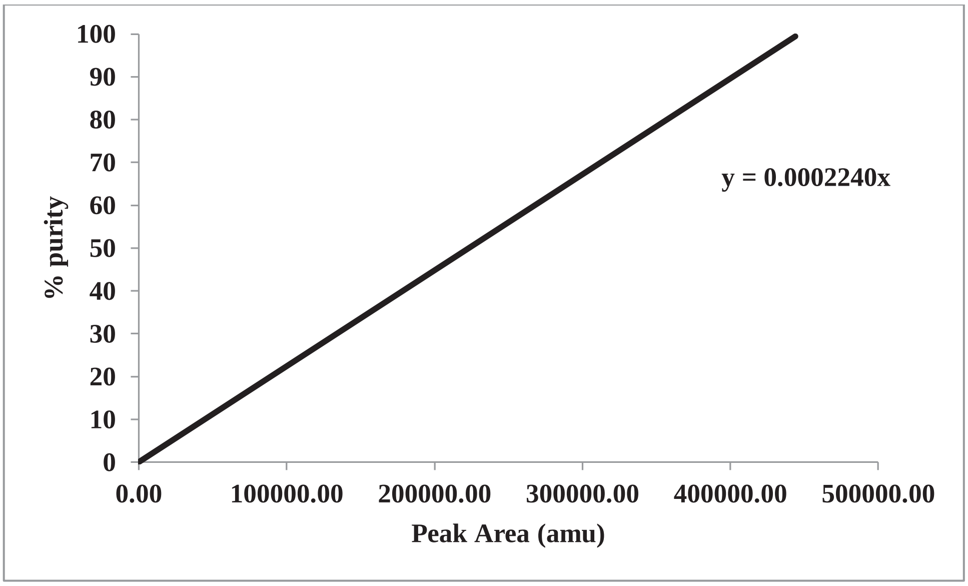

Figure C.3 Calibration curve for carbon monoxide 99.5%

APPENDIX D

CALCULATION OF METHANOL CONVERSION, HYDROGEN PRODUCTION RATE AND CO SELECTIVITY

APPENDIX D

CALCULATION OF METHANOL CONVERSION, HYDROGEN PRODUCTION RATE AND CO SELECTIVITY

The catalyst performance for the methanol steam reforming was evaluated in terms of activity for methanol conversion, Hydrogen selectivity and CO selectivity. As all components are gas phase so methanol conversion was defined as flow of C-component products such as CO_2 and CO occurred by methanol was converted with respect to flow of methanol in feed:

$$\text{Methanol conversion (\%)} = \frac{[flow\ of\ CO_2]+[flow\ of\ CO]}{[flow\ CH_3OH_{feed}]} \times 100 \qquad \text{D-1}$$

Flow of all components base on total flow from flow of nitrogen:

Basis : fixed bed reactor (in = out), nitrogen flow 100 ml/min.

$$\text{Find :} \qquad \text{Total flow} = \frac{flow\ nitrogen \times 100}{\%[nitrogen]} \qquad \text{D-2}$$

$$\text{Find :} \qquad \text{Flow of component} = [\frac{\%concentration \times total\ flow}{100}] \qquad \text{D-3}$$

By %concentration of all components obtained from computer program based plot on TCD (Poraplot U and molecular sieve 5Å). Calibrataion of each gas follow that :

D.1 Constant component from calibration curve

Components	**Constant**
H_2	0.0000227
N_2	0.000241
CO	0.000224
CO_2	0.0000975

So; % concentration = constant x average area D-4

Hydrogen production rate (mol/hr kg cat.) = $\frac{[flow\ of\ H_2]}{[g\ catalyst]} \times \frac{60\times1000}{22400}$ D-5

CO selectivity (%) = $\frac{[flow\ of\ CO]}{[flow\ CO+FlowCO_2]} \times 100$ D-6

APPENDIX F

INTERNATIONAL PROCEEDING

APPENDIX F

INTERNATIONAL PROCEEDING

<u>Nutcha Anurak</u>[a,], **Okorn Mekasuwandamrong**[a,*]**,** Kajornsak Faungnawakit[b]

"Nanostructured CuFe$_2$O$_4$ Spinel Catalysts Prepared by Flame Spray Pyrolysis for Hydrogen Production"

6th Asia Pacific Chemical Reaction Engineering Symposium (APCRE 2011), Beijing Chaina, 18-21 Sep, 2011. (oral presentation)

BIOGRAPHY

Name-Family name Miss Nutcha Anurak

Birthd Nov 7, 1986 in bankok, Thailand.

Address 24/213 Talardwhan District, Muange Amphur, Nonthaburi Province, Thailand, 11000.

Education Background

2008 received the bachelor degree of Chemical Engineering, Faculty of Engineering and Industrial Technology, Silpakorn University, Nakhon Phathom, Thailand.

2010 further studied in the master degree of Engineering, Department of Chemical Engineering, Graduate School, Silpakorn University, Thailand.

Special Interest Nanoparticles/Aerosol Technology/Heterogeneous Catalysis and Seperation